Quaternary Science Reviews xxx (2009) 1–19

Contents lists available at ScienceDirect

Quaternary Science Reviews

journal homepage: www.elsevier.com/locate/quascirev

Rapid and cyclic aeolian deposition during the Last Glacial in European loess: a high-resolution record from Nussloch, Germany

Pierre Antoine [a,*], Denis-Didier Rousseau [b,c], Olivier Moine [a], Stéphane Kunesch [a], Christine Hatté [d], Andreas Lang [e], Hélène Tissoux [d,f], Ludwig Zöller [g]

[a] Laboratoire de Géographie Physique, UMR 8591 CNRS, 1 Pl. A. Briand F-92195 Meudon Cedex, France
[b] Ecole Normale Supérieure, Laboratoire de Météorologie Dynamique, CERES-ERTI, UMR CNRS 8539, 24 rue Lhomond, 75231 Paris Cedex, France
[c] Lamont-Doherty Earth Observatory of Columbia University, Palisades, NY 10964, USA
[d] Laboratoire des Sciences du Climat et de l'environnement, CEA/CNRS/UVSQ, avenue de la Terrasse, 91198 Gif-sur-Yvette Cedex, France
[e] Department of Geography, University of Liverpool, Liverpool L69 7ZT, UK
[f] Département de Préhistoire du Muséum national d'Histoire naturelle, UMR 5198, 1 rue René-Panhard, 75013 Paris, France
[g] Lehrstuhl Geomorphologie, Universität Bayreuth, 95440 Bayreuth, Germany

ARTICLE INFO

Article history:
Received 2 July 2007
Received in revised form
27 July 2009
Accepted 3 August 2009

ABSTRACT

This paper reports the results of an investigation of the Weichselian Upper Pleniglacial loess sequences of Nussloch (Rhine Valley, Germany) based on stratigraphy, palaeopedology, sedimentology, palynology, malacology and geochemistry ($\delta^{13}C$), supported by radiocarbon, TL and OSL dating. Grain-size and magnetic susceptibility records are taken at 5 cm intervals from the Upper Pleniglacial (UPG) loess. The data indicate cyclic variations in loess deposition between ca 34 and 17 ka, when the sedimentation rate is especially high (1.0–1.2 m per ka for more than 10 m). The grain-size index (GSI: ratio of coarse silt *versus* fine silt and clay) shows variations, which are assumed to be an indirect measurement of wind intensity. The sedimentation rate, interpreted from the profiles, indicates high values in loess (Loess events LE-1 to LE-7) and low or negligible values in tundra gley horizons G1 to G8. OSL ages from the loess and ^{14}C dates from organic matter in the loess show that loess deposition was rapid but was interrupted by shorter periods of reduced aeolian sedimentation. Comparison between the data from Nussloch and other European sequences demonstrates a progressive coarsening of the loess deposits between ca 30 and 22 ka. This coarsening trend ends with a short but major grain-size decrease and is followed by an increase to a new maximum at 20 ± 2 ka ("W" shape). Correlation between the loess GSI and the Greenland ice-core dust records, suggests a global connection between North Atlantic and Western European global atmospheric circulation and wind regimes. In addition, the typical Upper Pleniglacial loess deposition begins at ca 30–31 ka, close to Heinrich event (HE) 3, and the main period of loess sedimentation at about 25 ± 2 ka is coeval to HE 2. Correlation of magnetic susceptibility and grain-size records shows that the periods, characterised by high GSI, coincide with an increase in the amount of ferromagnetic minerals reworked from the Rhine alluvial plain. They suggest enhancement in the frequency of the storms from N–NW. These results are integrated within a palaeogeographical model of dust transport and deposition in Western Europe for the Weichselian Upper Pleniglacial (or Late Pleniglacial).

1. Introduction

Grain-size variations in Chinese loess have been widely used as a proxy of past variations in both aeolian dynamics and patterns of monsoon development (Liu, 1985; Xiao et al., 1995; Vandenberghe et al., 1997; Fang et al., 1999; Ding et al., 1998, 2000, 2002, Vandenberghe and Nugteren 2001; Nugteren et al., 2004). In addition, evidence for rapid grain-size variations in Chinese loess deposited during the Last Glacial (L1 Loess) in the form of coarse peaks in median quartz values, has been interpreted by Porter and An (1995), as a possible consequence of Heinrich events defined in North Atlantic marine records.

Conversely, in western and central Europe, the numerous studies published on Last Glacial loess sequences have mainly been

* Corresponding author. Tel.: +33 (0)1 45 07 55 54; fax: +33 (0)1 45 07 58 30.
E-mail addresses: Pierre.Antoine@cnrs-bellevue.fr (P. Antoine), Denis.Rousseau@lmd.ens.fr (D.-D. Rousseau), Olivier.Moine@cnrs-bellevue.fr (O. Moine), Hatte@lsce.cnrs-gif.fr (C. Hatté), lang@liv.ac.uk (H. Lang), tissoux@mnhn.fr (H. Tissoux), Ludwig.Zoeller@uni-bayreuth.de (L. Zöller).

0277-3791/$ – see front matter © 2009 Elsevier Ltd. All rights reserved.
doi:10.1016/j.quascirev.2009.08.001

focused on stratigraphical correlations, palaeopedology, periglacial processes and dating (Sommé et al., 1980, 1986; Haesaerts et al., 1981, 2003; Haesaerts 1985; Lautridou, 1985; Zöller et al., 1988; Antoine et al., 1999, 2003a; Frechen, 1999; Frechen et al., 2003). Although a few discontinuous grain-size records have been obtained from European Weichselian loess sequences in Poland (Dolecki, 1986), Belgium (Vandenberghe et al., 1998) and the Czech Republic (Shi et al., 2003), their geochronological control is either weak (Dolni Vestonice, Shi et al., 2003), or controversial (Belgium, Juvigné et al., 1996).

Within this context, and in order to derive a detailed and well-dated record of grain-size variations, the authors decided to focus on the Weichselian Upper Pleniglacial (or Late Pleniglacial) loess sequences from Nussloch, Germany (Fig. 1A), where very high sedimentation rates and a complex stratigraphy have been identified (Antoine et al., 2001) (CNRS ECLIPSE Project EOLE). These two characteristics, associated with the particular situation of the site at the western edge of the Eurasian loess belt, provide ideal conditions for the investigation of the possible connections between dominant North Atlantic and Western Europe wind regimes.

In order to investigate these phenomena, a multidisciplinary study of loess–palaeosol profiles was begun in 1995 at Nussloch, in Germany. This study generated a detailed stratigraphical record of the Weichselian (Antoine et al., 2001, 2002). At this site, three main profiles were successfully investigated at high resolution and were correlated using well-defined stratigraphical markers such as palaeosols, erosion boundaries, periglacial horizons and a tephra layer. These investigations were supported by luminescence (TL, IRSL and OSL) and ^{14}C dating methods in order to provide a detailed geochronological framework, as well as a basis for intercomparison between various dating methods (Zöller et al., 1988; Zöller and Wagner, 1990; Hatté et al., 1998, 1999, 2001b; Lang et al., 2003; Tissoux et al., in press). Detailed stratigraphical, sedimentological, isotope, malacological evidences, together with a new method for precipitation estimates, were also recently published but are not addressed in this study (Antoine et al., 2001, 2002; Hatté et al., 2001a; Moine et al., 2002, 2005; Rousseau et al., 2002, 2007a; Hatté and Guyot, 2005).

The aims of the current paper are therefore:

(1) to synthesise all the new and previously presented high-resolution grain-size and stratigraphical results from the three profiles (P2, P3 and P4) from the Weichselian Upper Pleniglacial loess (UPG) at the site;
(2) to propose comparisons and correlations between these records and other grain-size records from European Weichselian Upper Pleniglacial loess sequences and from dust records derived from the Greenland ice cores.

2. Regional setting

The Nussloch loess and palaeosol sections are exposed within an active quarry about ten kilometres south of Heidelberg (49°18'59"N – 8°43'54"E), on the Kraichgau plateau, about 90 m above the alluvial plain of the Upper Rhine river (Fig. 1B). Previous sections in this huge quarry were first described by Sabelberg and Löscher (1978), and Bente and Löscher (1987). The P2, P3 and P4 profiles reveal up to 18 m of Weichselian loess and palaeosols which may be considered as a type sequence for Western Europe (Antoine et al., 2001, 2002; Rousseau et al., 2002, 2007a).

The study area lies on the eastern side of the Upper Rhine Graben, where a wide alluvial plain is developed at the bottom of the Kraichgau and Odenwald plateaux (Fig. 1B). During the Last Glacial Maximum this topography, in combination with strong NW winds (Lautridou, 1985; Antoine et al., 2001; Vandenberghe et al., 2006; Fig. 1A), favoured the accumulation of dust on the plateaux, close to the slope, in the form of 15–20 m thick by 2–4 km long NNW–SSE trending loess ridges, separated by small dry valleys (Fig. 1B). These features correspond to the 'gredas' described from

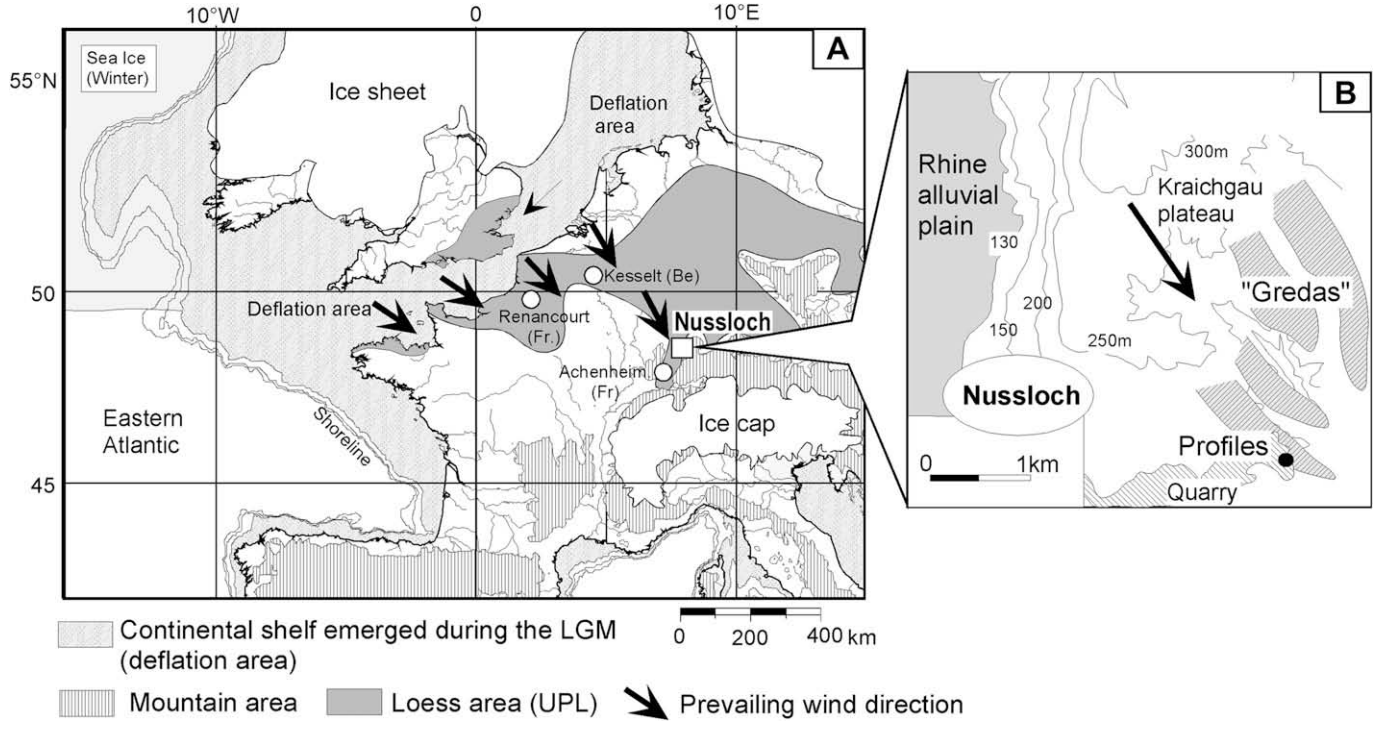

Fig. 1. Location of the Nussloch sequence within the north-Western European loess belt, based on Antoine et al. (2003a,b), modified, (ice sheets contours according to Svendsen et al., 2004, winter sea ice, according to Renssen and Vandenberghe, 2003).

Please cite this article in press as: Antoine, P., et al., Rapid and cyclic aeolian deposition during the Last Glacial in European loess: a high..., Quaternary Science Reviews (2009), doi:10.1016/j.quascirev.2009.08.001

Eastern Europe. The forms are orientated parallel to the direction of the prevailing winds (Léger, 1990). At Nussloch, the loess accumulation is favoured by the presence of the wide, braided alluvial plain of the River Rhine that developed during the Last Glacial Maximum (LGM) (Bibus, 1980; Brunnacker, 1986; Boenigk and Frechen, 2006). This braidplain provided the source of substantial volumes of sand and silt that were highly susceptible to deflation.

3. Stratigraphy and dating

Detailed analysis and correlation of the Nussloch profiles have revealed four sub-sequences (Antoine et al., 2001, 2002) (Fig. 2):

(I) a basal soil complex including a truncated brown leached soil, a grey forest soil and a steppe soil horizon,
(II) loess and aeolian sands (locally forming a dune),
(III) loess, brown soils horizons and tundra gley soils,
(IV) loess and tundra gley soils

Based on the complete set of dates obtained and on the climatic signature of the various soil horizons and sediment strata, these sub-sequences have been respectively attributed to:

(I) the Eemian Interglacial (MIS 5e) and Weichselian Early Glacial (MIS 5d-5a),
(II) the Weichselian Lower Pleniglacial (MIS 4),
(III) the Weichselian Middle Pleniglacial (MIS 3),
(IV) the Weichselian Upper Pleniglacial (UPG) (end of MIS 3 and MIS 2).

The best record of the topsoil has been observed in profile P6 (Fig. 2), located in a dry valley, at the bottom of the north-western slope of the loess ridge that also includes the P4 profile. At this locality, the topsoil is developed on reworked loess deposits (38e, Fig. 2) and covered by recent colluvial deposits.

Since this paper focuses on the grain-size records from the UPG sub-sequence, this part of the stratigraphy is described below. At Nussloch, the Weichselian Upper Pleniglacial (UPG) is represented by 10–13 m of calcareous loess that begins at the top of the upper boreal brown soil representing the uppermost unit of sub-sequence III (*Lohner Boden*, Fig. 2), as in other sections in the Rhine Valley (Zöller et al., 1988; Semmel, 1997; Frechen, 1999). The UPG calcareous loess shows no signs of weathering, other than numerous more or less cryoturbated tundra gley horizons (G), some of which have gelifluctate at their surface (Gelic Gleysols). The typical loess-ridge morphology of the area is composed of UPG loess, so that the transverse section through the loess ridge that provided P4 (Fig. 3A) demonstrates that the palaeotopography of the *Lohner Boden*, located halfway up the profile, is almost horizontal. In contrast that of the Eltviller Tuff, that occurs close to the top of the profile, is almost parallel to the modern surface topography and reflects the relief of the ridge.

The UPG sequence can be divided into three parts from the base upwards (Fig. 2):

A basal member (units 21–23; maximum thickness: ~2 m), showing several homogeneous calcareous loess units and cryoturbated tundra gley layers (*Nassboden*, Fig. 3E) dated ca 31–30 ka by IRSL and ^{14}C in P2 and P4 profiles.

A median member (units 24–35; maximum thickness: ~7 m) mainly composed of finely laminated calcareous loess (Fig. 3C), with cryo-dessication micro-cracks and cryoturbated tundra gley soils in the lower part (Fig. 2). IRSL dates from this unit indicate that the laminated loess began to form from ca 30 to 29 ka and comprise millimetre-thick fining-upward micro-sequences (sand, coarse loess, then loess), intercalated with levels of fine cryo-dessication micro-cracks. These laminated loesses (Antoine et al., 1999, 2003b) show characteristics typical of niveo-aeolian deposits (Sommé et al., 1980, Haesaerts, 1985).

The upper part of laminated unit 34 includes a volcanic ash layer (Fig. 2: E.T), which has been correlated with the Eltviller Tuff (Juvigné and Semmel, 1981). At Nussloch, this has been dated to ~22 ka by TL (Zöller et al., 1988), 21.13–22.16 by ^{14}C (Hatté et al., 2001b), 19.2 ± 1.7 ka (below) and 19.5 ± 1.3 ka (above) by IRSL (Lang et al., 2003) and recently to 23.0 ± 1.8 (below) by OSL (Tissoux et al., in press).

An uppermost member (units 36–38; maximum thickness: ~4 m) including homogeneous loess and incipient gley layers is homogeneous loess, separated from the underlying laminated loess by a greyish gley horizon with deformed cracks caused by gelifluction. This soliflucted Gelic Gleysol (G7), overlain by a loess layer dated to 20.8 ± 1.8 ka by IRSL, is likely to represent a local signature of the well-known Nagelbeek–Kesselt 'tongue horizon', described in west-European loess series between the two main UPG loess bodies (Haesaerts et al., 1981). Based on the available IRSL and ^{14}C dates, the end of the UPG loess sedimentation can be dated to ca 18–17 ka (Lang et al., 2003, Bibus et al., 2007). The absence of the youngest part of the UPG is explained by erosion that probably occurred during the Lateglacial and the Holocene, as shown by the sharp boundary that occurs between the loess and the reworked topsoil in P4 (Fig. 2). This interpretation is reinforced by the occurrence of re-deposited loess at the base of profile P6 at the bottom of the dry valley (profile P6, 38e, Fig. 2).

4. Material and methods

4.1. Stratigraphy and sampling

The three main loess profiles P2, P3 and P4, situated in two neighbouring loess ridges, were investigated in the Nussloch quarry between 1997 and 2006. A detailed plot (scale 1: 20) showing the precise location of all the samples was made for each profile after careful cleaning (Fig. 2). The detailed investigation of these three Upper Pleistocene profiles allowed the definition of 40 stratigraphic units.

4.2. Grain size

Grain-size samples were collected from profiles P2 and P3 at 10 cm intervals using a hand coring system (tube: ø 4 cm) hammered in the loess exposure. A new technique based on the careful cutting of a continuous loess column or monolith (±5 cm wide) was later used in P4 and P6 profiles to produce a continuous record of the grain-size variability every 5 cm (Fig. 3B). This sampling method, termed 'CCS' (*Continuous Column Sampling*), eliminates gaps in the grain-size record, which might arise from collection of a series of isolated samples.

The P2 profile was analysed using the classical method of sieving and pipetting without decalcification. Analysis was carried out on 10 g homogenised sub-samples, after sieving at 200 μm to remove the coarse fraction (e.g. $CaCO_3$ and Fe–Mn concretions, calcified rootlets, mollusc shell fragments). Removal of the organic matter and dispersion of particles was achieved using H_2O_2 followed by ultrasound, following addition of sodium hexametaphosphate. The following grain-size classes were determined (INRA Standard: NF-X-31-107): clay (<1 μm); clay (1–2 μm); fine silt (2–20 μm); coarse silt (20–50 μm); fine sand (50–200 μm) and coarse sand (200–2000 μm) (Antoine et al., 2001).

For profiles P3, P4 and P6, particle size distributions were determined using a Beckman-Coulter LS 230 laser particle sizer (LPS), from 10 g homogenised sub-samples dispersed by sodium

Please cite this article in press as: Antoine, P., et al., Rapid and cyclic aeolian deposition during the Last Glacial in European loess: a high..., Quaternary Science Reviews (2009), doi:10.1016/j.quascirev.2009.08.001

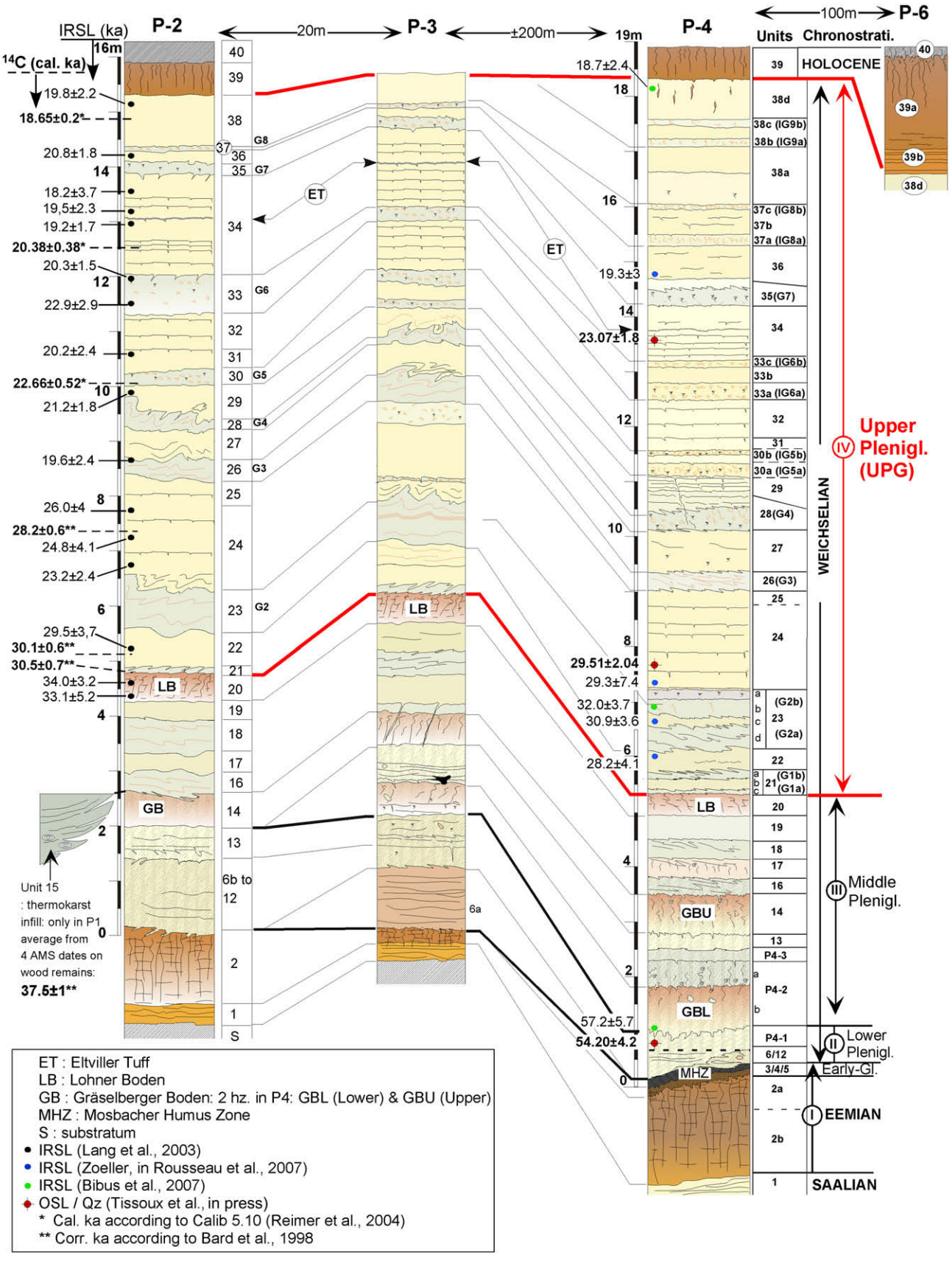

Fig. 2. Detailed stratigraphy of the Nussloch loess section profiles P2, P3, P4 and P6, (according to Antoine et al., 2001, 2002, modified). 1 – Calcareous (Saalian), 2a and 2b – Truncated brown leached soil (Eemian), 3–5 (Early Glacial) Grey forest soil on colluvium (3/4), 5 – Humic steppe soil, 6a – Laminated sandy-loamy colluvium, (Units 7–12 not described here: only observed in profile P1, see Antoine et al., 2001), 13 – Aeolian sands P4-2, 14 and 20: Boreal brown soil horizons (Cambisols) (Middle Pleniglacial), 16 and 18: Tundra gley (Middle Pleniglacial), 17 and 19 (homogeneous calcareous loess (Middle Pleniglacial), 21–38: Upper Pleniglacial loess sequence (UPG): homogeneous loess (22, 23c, 31, 33b, 36, 38a, d), main tundra gley horizons (21, 23a, b, d, 26, 35), Incipient tundra gleys (30a,b, 33a,c, 37a,c, 38b,c), laminated loess with cryo-dessication micro-cracks (24, 27, 29, 32, 34). 39-40: surface soil (Lateglacial and Holocene).

Please cite this article in press as: Antoine, P., et al., Rapid and cyclic aeolian deposition during the Last Glacial in European loess: a high..., Quaternary Science Reviews (2009), doi:10.1016/j.quascirev.2009.08.001

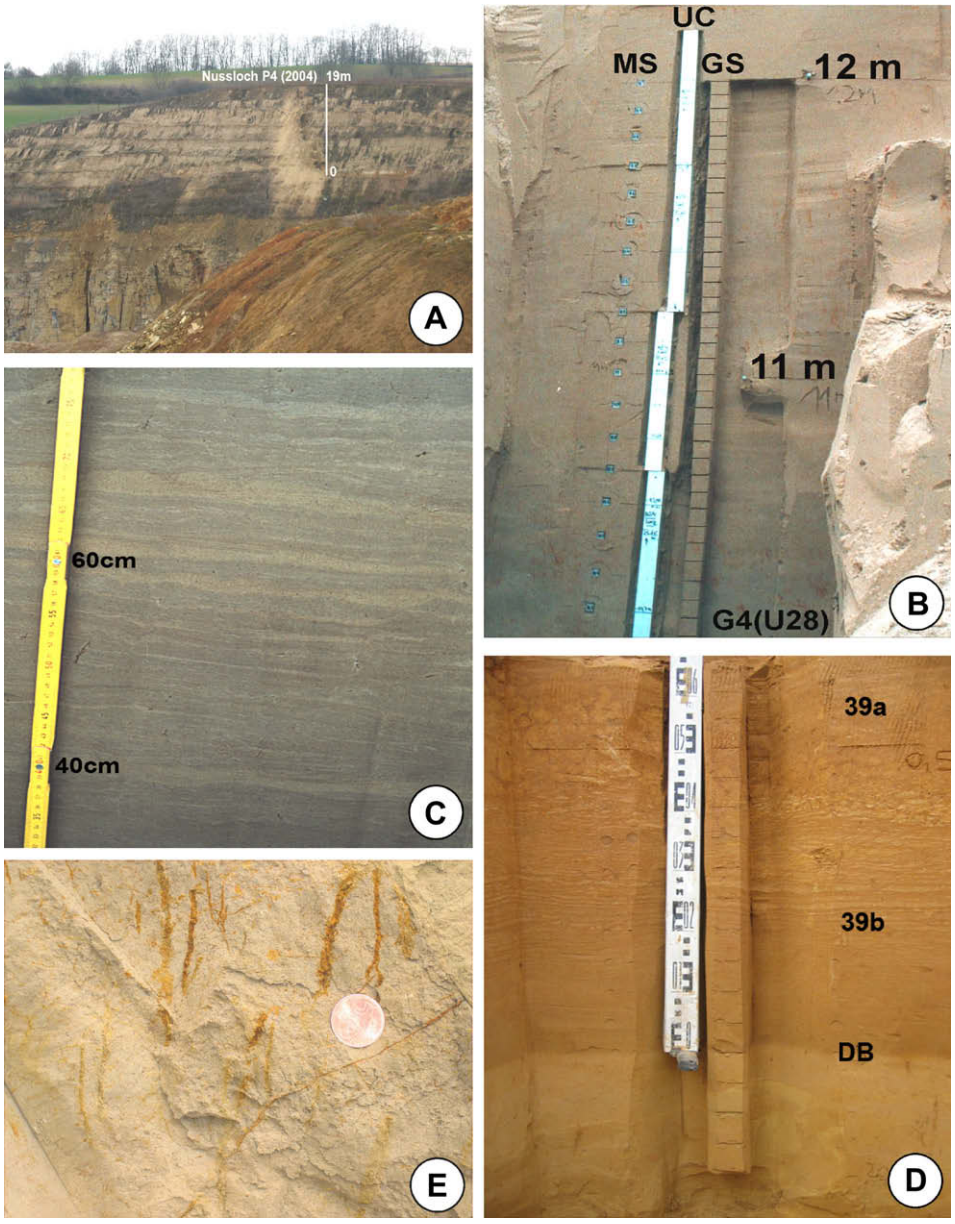

Fig. 3. (A) – General view of the section of the loess 'greda' and underlying formations in the Nussloch quarry (2004), and position of the main profile Nussloch P4. (B) – Nussloch profile P4: continuous high-resolution sampling method ('CCS': Continuous Column Sampling/EOLE project); GS: Grain size, MS: Magnetic susceptibility, UC: U Channels (grey level analysis/loess magnetism). (C) – Nussloch profile P4: laminated loess facies, including single aeolian sand beds (see Fig. 2, Unit 24). (D) – Nussloch profile P6: base of the topsoil sequence (total thickness: 2 m), including upper Bt horizon (39a), lower banded Bt ('doublets horizon', 39b) and decalcification boundary (DB). (E) – Oxidised root tracks within the tundra gley layer G2a (see Fig. 2: unit 23b) (coin: 2 cm).

hexametaphosphate. The samples were treated over a period of 2 hours in a rotating agitator (400 ml/10 g), and then sieved at 160 μm to remove the coarse fraction. The measurements have been repeated at least three times in order to obtain good reproducibility. After dispersion of the sediment, two analyses are performed by pipetting to obtain a saturation value between 8% and 12% for the PIDS (difference in diffusion of the polarised intensity) and between 45% and 55% for the whole sensors. The optical model takes into account the refraction indices of water ($n_D = 1.333$ at 20 °C) and of the sediment ($n_S = 1.64$), and the absorption coefficient of the sediment particles ($a = 0.1$). For each profile, the calibration of the results provided by the LPS was performed by applying both LPS and classical analysis on a set of 10 test samples originating from a range of stratigraphical units. Thus, the classical limits of grain-size classes at 2, 20 and 50 μm used with the sieve and pipette method, respectively correspond to LPS limits at ca 4.6 μm, 26 μm and 52 μm applied to the Nussloch sample analysis. These results are in agreement with the observations published by Konert and Vandenberghe (1997).

A grain-size index (GSI), defined as the ratio between coarse loam and fine loam plus clay, has been found to be the most effective way of highlighting grain-size variations after numerous experiments throughout the Upper Pleniglacial loess (UPG). According to the previous calibration of the LPS results, the GSI ratio for both methods is defined as follows:

GSI for classical method: (% 20–50 μm)/(% <20 μm) (P2 profile)
GSI for LPS: (% 26–52 μm)/(% <26 μm) (P3, P4 and P6 profiles)

Please cite this article in press as: Antoine, P., et al., Rapid and cyclic aeolian deposition during the Last Glacial in European loess: a high..., Quaternary Science Reviews (2009), doi:10.1016/j.quascirev.2009.08.001

4.3. Magnetic susceptibility

Low field magnetic susceptibility has been measured *in situ* in the three profiles using a MS2F portable Bartington Susceptibility Meter (10 measurements averaged for each level). Cubic samples ($2 \times 2 \times 2$ cm dimensions) were taken at the same levels as laboratory measurements (Fig. 3B).

4.4. Dating methods

^{14}C dating was mainly carried out on samples of organic material from profiles P2 and P4, and also on wood remains and bones in P1 profile. The detailed protocol is presented in Hatté et al. (2001b).

IRSL measurements were carried out on 16 samples from P2, and 13 samples from P4 (only the 5, analysed so far are shown in Fig. 2). The dosimetry was measured from sediment samples using high-resolution gamma spectrometry (Lang et al., 2003; Rousseau et al., 2007a).

OSL dating (P4) was carried out on the 32–63 μm quartz fraction extracted by wet sieving. The measurement of the radioactive elements contents (U, Th and daughters and K), were performed *in situ* with a gamma spectrometer using a high-purity germanium detector (GeHP). Water content was estimated by weighting the sediment before and after drying for 3 days at 120 °C (see Tissoux et al., in press for the presentation of the detailed protocol).

5. Results

5.1. Grain size, magnetic susceptibility and sedimentation rates

5.1.1. Grain size

The mean percentages of the main grain-size classes throughout the 10 m-thick UPG loess of profile P2 (100 samples from unit 22 to 38, Fig. 2) are: clay: 9.2%; fine silt (2–20 μm): 23.5%; coarse silt (20–50 μm): 58.7%; fine sand (50–200 μm): 7.9%; coarse sand (200–2000 μm): 0.67%; and the mean $CaCO_3$ is 23.8% by weight.

A comparison of a continuous sequence of 32 test samples from P4 was performed both before and after decalcification by HCl. The results are very close (correlation coefficient = 0.962) showing that, in the case of typical loess, preliminary decalcification is unnecessary prior to grain-size analysis (Fig. 4). Thin sections from the Nussloch loess show that detrital $CaCO_3$ represents about 20% of the sediment mass, and is dispersed through all grain-size classes (Antoine et al., 2001).

The continuous grain-size records from the main three profiles (P2, P3 and P4) show similar rapid and cyclic variations throughout the UPG loess (Figs. 5–7). These profiles can be accurately correlated with each other despite the use of different analytical techniques (Fig. 8: $r_{P2/P4} = 0.79$; $r_{P3/P4} = 0.88$). This observation validates the reproducibility of grain-size records, the quality of the results and thus the authors' methodology. Consequently, all descriptions will be based on the P4 profile, which is the most complete and characterised by the highest sampling resolution. Mention will be made to other records where relevant.

5.1.1.1. General trends. Throughout the UPG loess (excluding the Lohner Boden), the variation ranges of the main grain-size classes can be summarised as follows (Figs. 5–7):

- The clay fraction varies between 7 and 13% in P2 (<2 μm), 6 and 12% in P3 and 5 and 13% in P4 (<4.6 μm).
- The coarse silt fraction varies between 55 and 67% in P2 (20–50 μm), 35 and 45% in P3, 35 and 47% in P4 (26–52.6 μm).
- The fine sand fraction (50–200 μm) varies between 4 and 19% in P2, 13 and 31% in P3, 7 and 27% in P4 (63–160 μm).

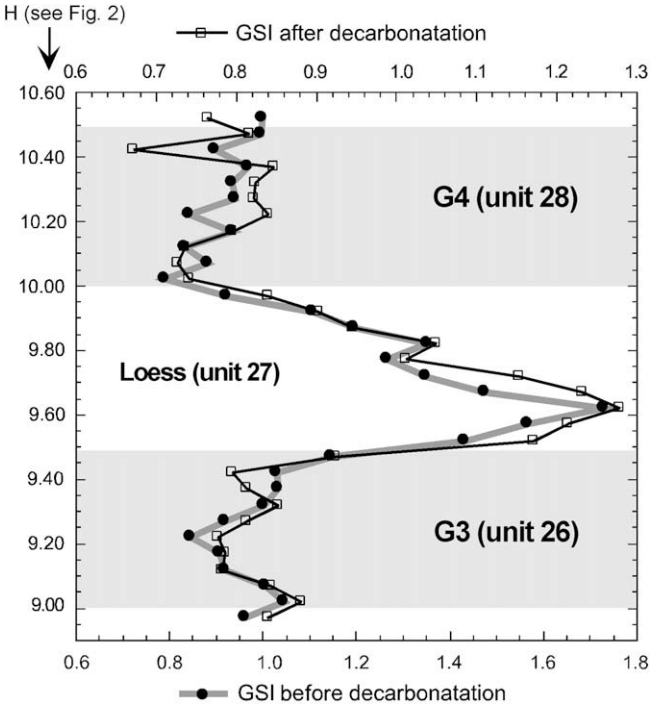

Fig. 4. Nussloch profile P4: comparison between the variation of the GSI before and after decarbonation from +9.00 to +10.55 m (see Fig. 2 for location within the whole section).

- The GSI varies between 0.4 and 3 in P2, 0.5 and 1.5 in P3 and 0.5 and 1.9 in P4.

Despite small variations in the grain-size values and GSI, as a result of different analytical techniques, the general trend of both the GSI and the fine sand fraction is similar and characterised in the three profiles by an increase from the Lohner Boden (unit 20) to the top of loess unit 34. It is then followed by a strong decrease from G7 to G8 (units 35–37), and a further increase in the upper loess unit 38 (Fig. 8).

The clay fraction values show an inverse relationship to both the fine sand percentage and GSI. Because human activity has reworked the soil at the top of the loess ridge, including P4 (Fig. 3A), the topsoil was only sampled in P6 profile, where it is 2 m thick. Here the clay content varies from 14% in the lower banded horizon (Fig. 3D) to 25–29% in the upper typical Bt, which is similar to the maximum of 27% measured in P2 topsoil. This *in situ* Bt horizon (unit 39a, Fig. 2) is also characterised by low GSI values (0.4–0.5).

5.1.1.2. Evidence for a cyclic pattern within the UPG loess. A cyclic saw-tooth pattern is superimposed on these general trends, and reflects shorter variations in grain-size and GSI values (Fig. 7). This pattern closely relates to the alternation of loess and gley units within the UPG loess sequence. Compared to pure loess, the tundra gley soils (G) are characterised by lower GSI values and higher clay percentages (10–12% for gleys vs. 7–8% for loess). This correlation is particularly clear in the lower part of the UPG sequence, where the tundra gleys G1–G4 are thicker and better recorded in the stratigraphy. This observation forms the basis of the definition of seven cycles (C-1 to C-7) for the whole UPG loess sequence (Fig. 7). Cycles C-2 to C-6 are well expressed and bracketed by two shorter ones, C1 and C7, respectively at the base and at the top of the UPG sequence (Fig. 7). Each cycle extends between particularly well-marked minima in the GSI, or maxima in the clay fraction, associated with

Please cite this article in press as: Antoine, P., et al., Rapid and cyclic aeolian deposition during the Last Glacial in European loess: a high..., Quaternary Science Reviews (2009), doi:10.1016/j.quascirev.2009.08.001

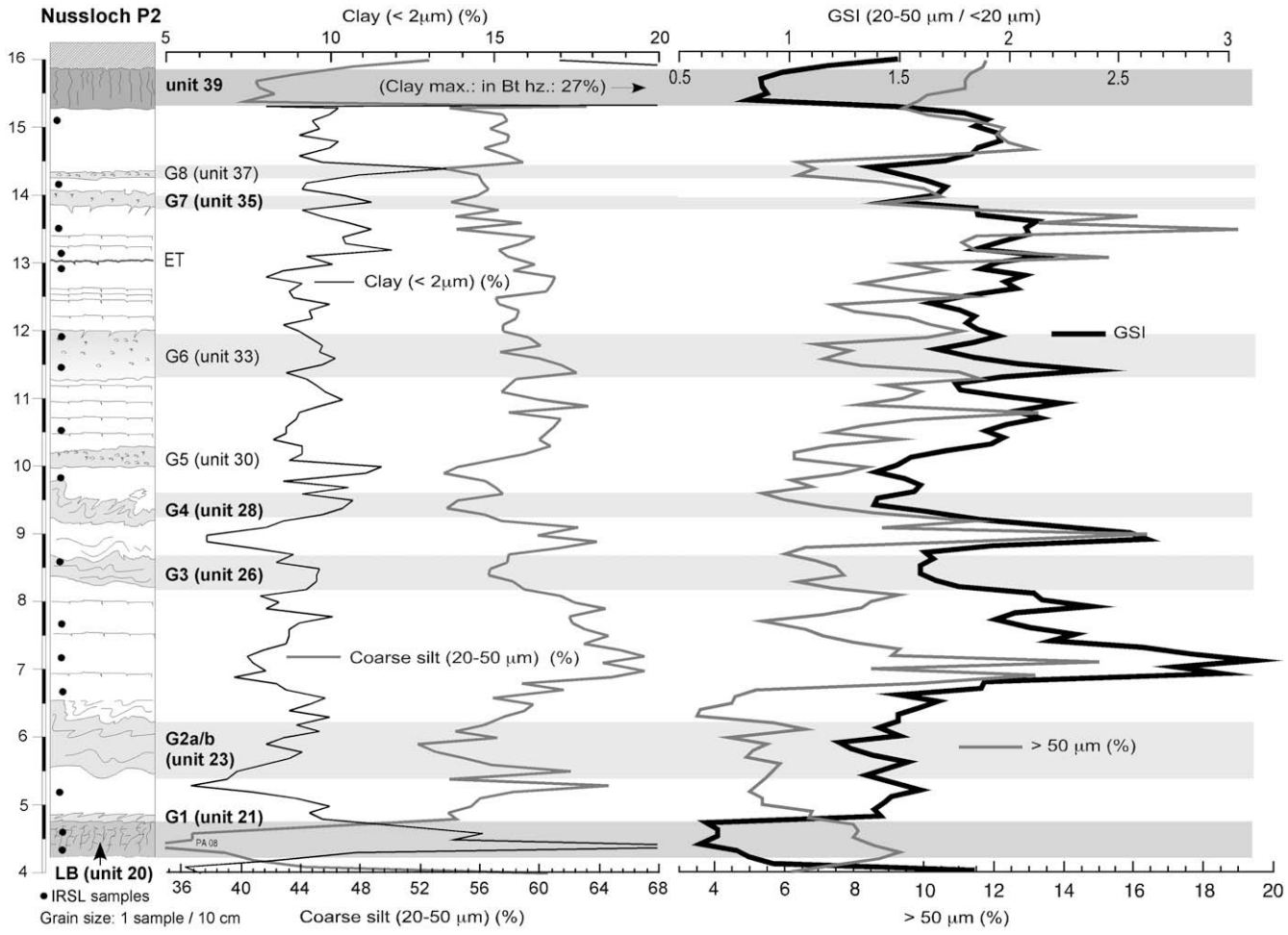

Fig. 5. Nussloch profile P2: main grain-size data (see text for details).

tundra gleys. The shape of each cycle is different in detail, depending on the combined influence of stratigraphy and fluctuations in the sedimentation rate. Cycles C-1, C-4, C-5 and C-7, show a progressive increase in the GSI and percentage sand followed by a rapid decrease, while C-6 shows an inverse pattern and C-2 and C-3 show a symmetrical pattern. The clay fraction signal shows a pattern that is the inverse of the fine sand fraction, and with a similar relative magnitude. Consequently, they are not considered in the remainder of the paper.

Finally, Loess Events (LE) have been named to highlight the main episodes of coarser loess deposition that appear in the three profiles (high GSI and high percentages in fine sands). Each Loess Event occurs within a C-cycle, i.e. LE 3 occurs in cycle C-3 and so on (Fig. 7).

Cycle C-1: The first cycle is defined between the top of the Lohner Boden (LB) and the base of the first well developed tundra gley (G2a, unit 23d, Fig. 7). C-1 is not as well expressed as the following cycles, owing to a lower sedimentation rate at the beginning of the UPG at ca 32–31 ka. C-1 begins within the Lohner Boden, with the lowest GSI values, reaching a maximum in loess unit 22 and ends at the base of G2a (unit 23d). C-1 has not been divided into subcycles since it has a limited range in grain-size and a low sedimentation rate.

Cycle C-2: The second cycle begins in G2a (unit 23d), where the sedimentation rate is still rather low and ends within G3 (unit 26). C-2 is characterised by the first substantial increase in GSI, which occurs in the lower half of the laminated loess unit 24. C-2 ends with a two-step decrease, respectively in the middle and at the top of loess unit 24. Like C-1, and for the same reasons, C-2 has not been divided into subcycles.

Cycle C-3: Being about 1.5 m thick, the third cycle is the thinnest. It is, however, well expressed as a consequence of very strong variations in the grain-size parameters. C-3 begins within G3 (unit 26), reaches a GSI maximum in the middle of loess unit 27, and then decreases rapidly to the base of G4 (unit 28). In the three profiles, the more or less symmetrical shape of both GSI and fine sand fraction records provides a grain-size marker in the Nussloch sequences (Fig. 8).

Cycles C-4 and C-5: The fourth and fifth cycles are characterised by an asymmetrical shape, resulting from the increasing values of both GSI and fine sand proportions, which are only disturbed by a short and sharp decrease at the base of gley G6a.

C-4 begins at the base of G4 (unit 28), reaches a maximum in the laminated loess unit 29a, and ends at the basis of G6a (unit 33a).

C-5 shows an irregular increase in both GSI and fine sand values up to a maximum within laminated loess unit 34. This is followed by a very sharp drop on both indicators within G7 (unit 37), which is the last well developed tundra gley of the sequence. C-5 ends a few decimetres above G7 in P4.

Cycle C-6: The sixth cycle begins with a rapid increase in both GSI and the fine sand fraction within loess unit 36, and continues by a progressive and irregular decrease to a new minimum at the top of a weakly oxidized layer (G9a, unit 38b). Unlike the previous cycles this has a plateau shape rather than a sharp maximum.

Please cite this article in press as: Antoine, P., et al., Rapid and cyclic aeolian deposition during the Last Glacial in European loess: a high..., Quaternary Science Reviews (2009), doi:10.1016/j.quascirev.2009.08.001

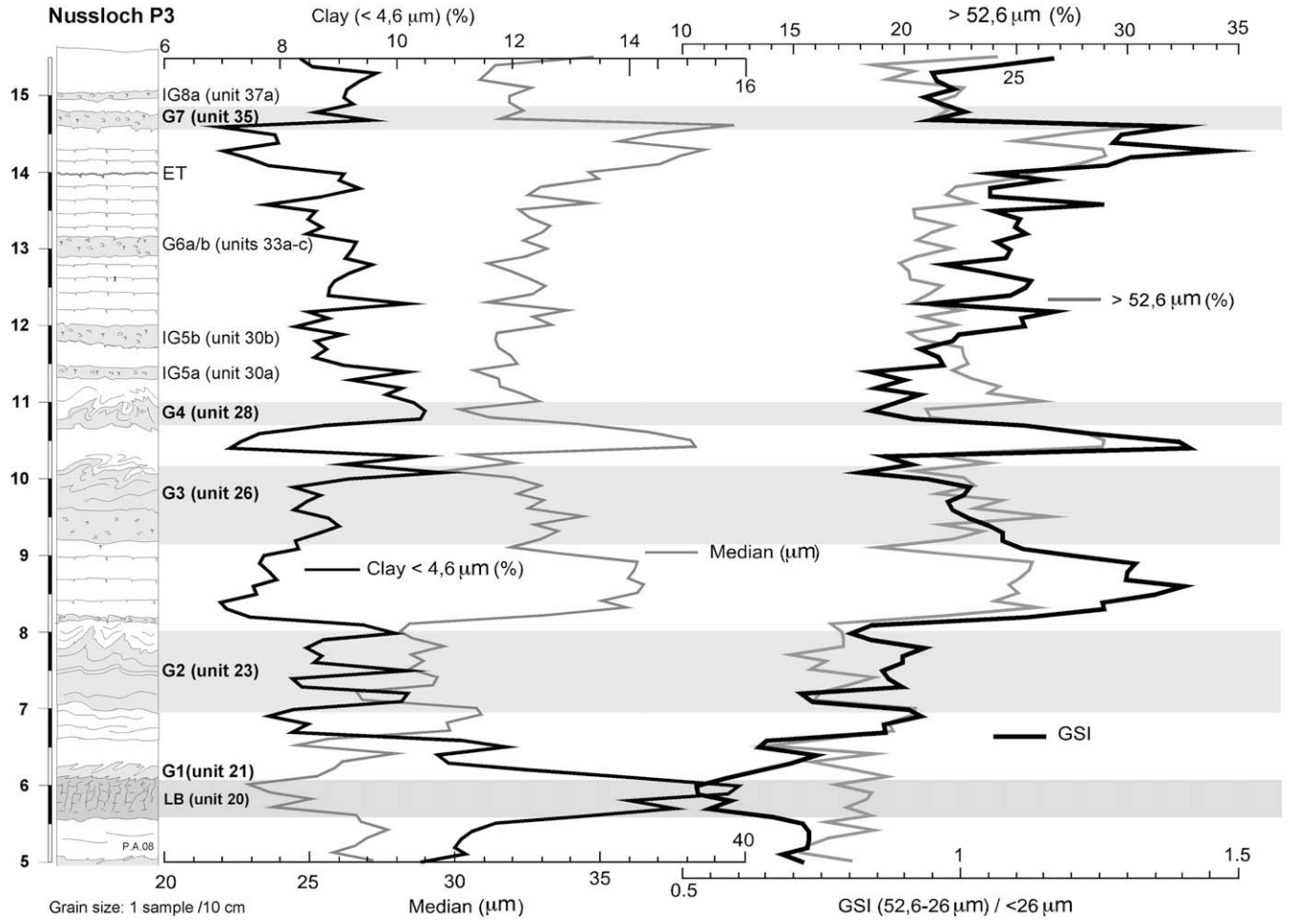

Fig. 6. Nussloch profile P3: main grain-size data (see text for details).

Cycle C-7: The seventh cycle extends from the top of the thin gley G9a (unit 38b) to the base of the topsoil. The shape of C-7 is difficult to characterise because it is truncated at the base of the topsoil, and the uppermost values of the GSI are artificially low as a result of clay enrichment caused by the topsoil development.

Both the general trends and main cyclic variations are well expressed in the grain-size records from profiles P2, P3 and P4 (Fig. 8). The resulting pattern of these records can be considered as a reference for grain-size variations throughout the UPG loess sequence of Nussloch.

5.1.1.3. Subcycles. The high-resolution P4 grain-size record reveals also a number of very short cycles superimposed on the general trends and main cycles. These fine rhythmic units are ~0.25–0.3 m thick and occur throughout the whole UPG loess sequence, and are especially well developed between 12 and 14 m in units 29–34, where they show a magnitude of 3–5% in the fine sand, 2–3% in the clay fraction percentages and 0.2–0.3 units in GSI (Fig. 7). Moreover, most of the layers from incipient gleys (IG5, IG6, IG8 and IG9), with a slightly greyish colour and oxidised root tracks and pseudomycelium (Fig. 2), are correlated with GSI minima in these shorter cycles (Fig. 7).

Finally, the variations in grain size are more frequent in the laminated loess of units 24–34, and especially within unit 24. Field observations and thin sections demonstrate that unit 24 (Fig. 2) has fine laminations comprising thin layers of sand and sandy loess forming fining-upward sequences. The thickness of these sequences varies from 2 to 5 mm but can reach up to 1 cm (Fig. 3C). A grey level analysis of these laminated loess, using a scanner and NIH Image software (Bond et al., 1993), clearly reveals the lithological contrasts responsible for the laminated facies of this loess unit (Antoine et al., 2003a).

5.1.2. Low field magnetic susceptibility (MS)

Throughout the Nussloch profiles, in common with other Upper Pleistocene loess sequences from north-western France (Rousseau et al., 1994, 1998; Antoine et al., 2003b), the highest MS values are systematically recorded within the Weichselian Early Glacial soil complex (Bth horizons of grey forest soils and Ah horizons of steppe soils, Fig. 2 units 3–5) and the Holocene topsoil, whereas lowest MS values are typical of allochtonous loess units (Antoine et al., 2001).

Except at the level of the Eltviller Tuff, where MS values are high in each profile (16.5 SI units in P2 and 31 in P4), the mean MS values throughout the UPG loess and gley sequence are low: 7.43 SI units in P2, and 8.59 SI units in P4. Since the profiles P2 and P4 are very similar, the description of the main features of their MS record will be based on the P4 data. Throughout profile P4, MS values vary between 6 and 14 SI units, including pronounced peaks within typical loess events LE-1b, LE-2b and two less pronounced peaks, in loess events LE-3 and LE-4. The MS record can be divided into a lower part, from LE-1a to G4, showing wide variations (4–5 SI units in magnitude), and an upper part, from the base of LE-4 to LE-7, showing small variations (2–3 SI units in magnitude). Both the MS record and stratigraphy show a close correspondence from the top of the Lohner Boden to G4, which is characterised by higher MS values within pure loess units, and lower ones within tundra gleys

Please cite this article in press as: Antoine, P., et al., Rapid and cyclic aeolian deposition during the Last Glacial in European loess: a high..., Quaternary Science Reviews (2009), doi:10.1016/j.quascirev.2009.08.001

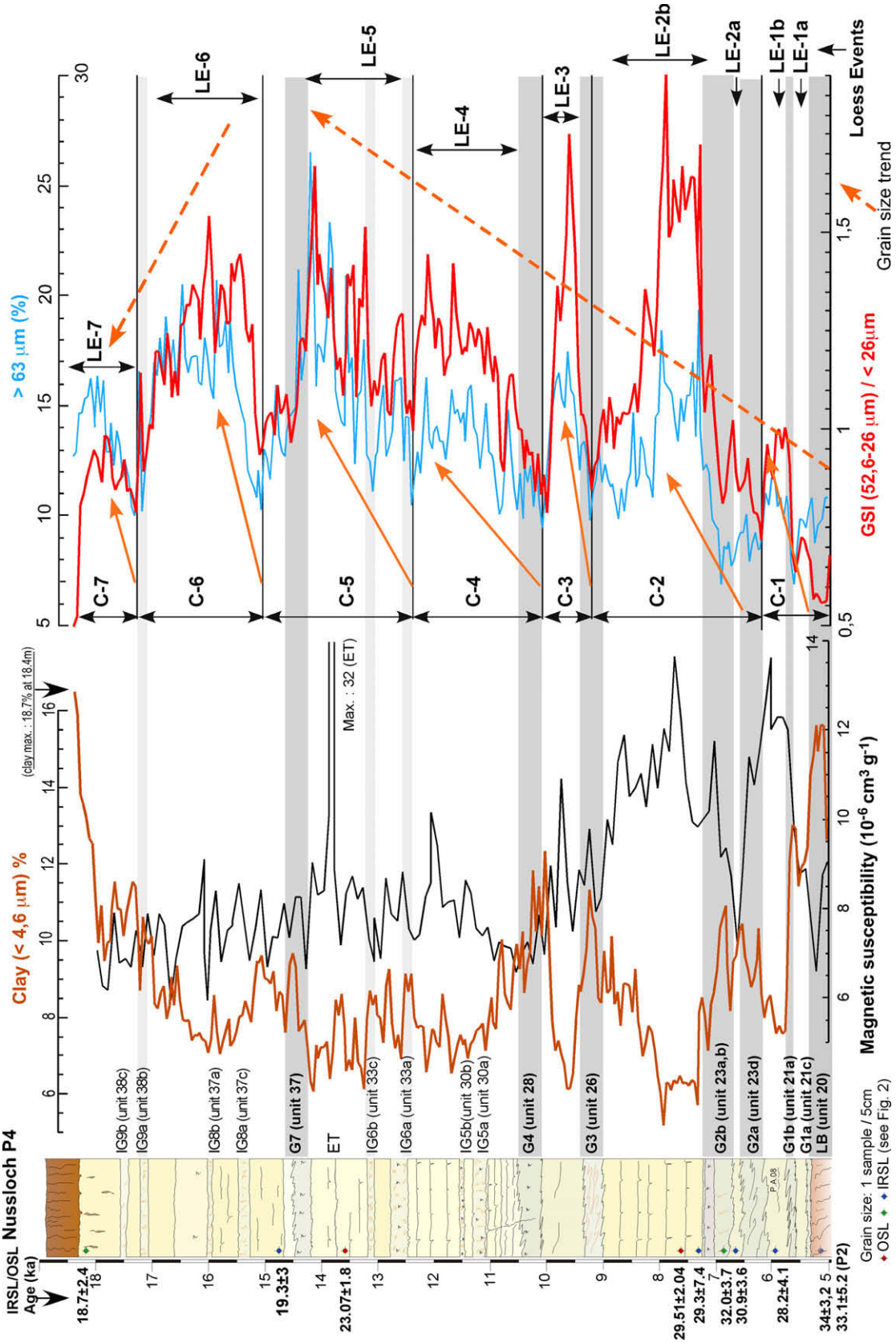

Fig. 7. Nussloch profile P4: main grain-size data and magnetic susceptibility (see text for details), definition of grain-size cycles and of 'Loess Events' (LE). The dashed arrows indicate the main grain-size trends.

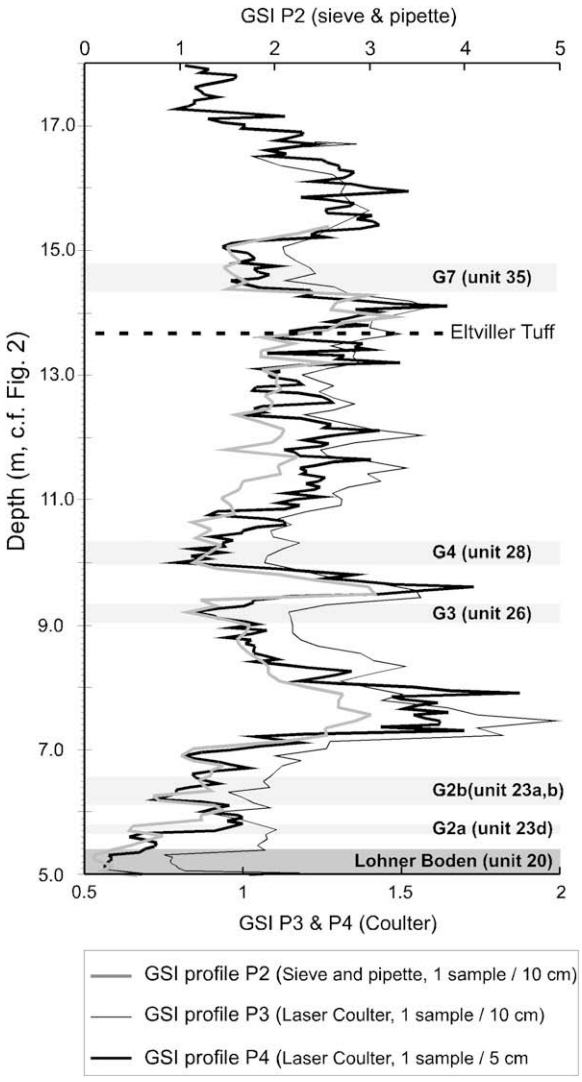

Fig. 8. Correlation between the GSI curves of the three profiles (according to Rousseau et al., 2007a, modified). Correlation between the GSI curves of the three profiles studied. GSI curves for profiles P1 and P3 are tuned to P4 depth with Analyseries software (Paillard et al., 1996) by using all correlated boundaries determined for the three different sequences. The position of the Eltviller Tuff was not used in the tuning but for testing its reliability. Main tundra gley layers are represented by horizontal grey bands, according to their position in profile P4 (with corresponding unit numbers).

G1–G4 (Fig. 7). The upper part of the MS record shows no general trend and no particular correlation with the stratigraphy.

The comparison with the grain-size data shows that only the four distinct MS increases of loess events LE-1b, LE-2b, LE-3 and LE-4 are synchronous with GSI increases, even if the shape and magnitude of these increases differ between both proxies. Consequently, the main MS variations can hardly be precisely linked with the previously defined grain grain-size cycles C-4 to C-7, and it cannot be excluded that the shorter cyclical variations in MS may result from measurement inaccuracy arising from technical limitations of the probe.

6. Discussion

6.1. Tundra gley layers (G): synthesis and development model

The tundra gley soils (Gelic Gleysol), that are developed throughout the UPG loess sequence, correspond to those occurring during the same period in the Belgian and French loess series (Haesaerts and Van Vliet-Lanoë, 1974; Van Vliet-Lanoë, 1987; Antoine et al., 2003a,b) and to the *Erbenheimer Nassboden* E1 to E4/E5 of German authors (Semmel, 1997; Schirmer, 2000). Therefore, tundra gley horizons provide good stratigraphical markers within Upper Pleniglacial loess sequences of Western Europe.

In the well-known Harmignies loess sequence (Belgium), they have been allocated to a cold and humid environment (permafrost) because of the occurrence of cryo-injections and ice wedges (Haesaerts and Van Vliet-Lanoë, 1974, 1981; Van Vliet-Lanoë, 1987). On the other hand, the tundra gleys described in the Kesselt (Belgium) loess sequence, have been attributed by Vandenberghe et al. (1998) to short interstadial periods characterised by finer loess deposition and more intense biological activity (Vandenberghe and Nugteren, 2001).

According to the new observations from Nussloch (using field observations, thin sections, sedimentological data, molluscs), these gley soils were formed by hydromorphic processes: water-logging, reduction of iron, slight decalcification with redistribution of carbonates at the base of the profile (small loess concretions), reduction and redistribution of iron (oxidised patches and bands). They are also marked by a slight increase in total organic carbon (TOC: G2: 0.25%, G4: 0.13%, P2 UPG loess average: 0.064%), more root development (Fig. 3E) and biological activity, indicated by an increase in the number of mollusc shells and of earthworm biospheroids and burrows (mainly at the top).

Terrestrial mollusc faunas, although more abundant than in the pure loess, are represented by open-environment associations dominated by species such as *Pupilla muscorum*, *Trochulus hispidus* and *Succinella oblonga*. However, the proportion of the hygrophilous species *Succinella oblonga* rises sharply at the top of tundra gley soils and the proportions of species preferring dry conditions decreases (Moine et al., 2008). There is also a sharp increase in the abundance of all mollusc species at the top of thickest tundra gleys (G1–G4) that indicates warmer temperatures (Moine et al., 2008).

Additionally, verification of a rapid climatic improvement can be seen from the evidence of the decay of ice wedges and gelifluction of the active layer observed in a number of west-European sequences (Antoine et al., 1999, Antoine et al., 2003a). This interpretation is re-enforced by evidence from slopes that show deep incisions arising from the rapid melting of permafrost (thermokarst). These processes have been described from the Villiers-Adam section (Paris Basin), at the base of the UPG loess (Antoine et al., 2003a), and in the Nussloch profile P1, during the Middle Pleniglacial, before the deposition of the organic layered sediments of unit 16 (Fig. 2; Antoine et al., 2001). In both cases, casts of former ice wedges have been detected at the base of the incisions.

On the basis of the latest observations from Nussloch, the tundra gley horizons are thus interpreted to result from both incipient soil formation and active-layer deepening processes, that operated during short periods of reduced aeolian sedimentation ($<$1 ka). Based on the evidence presented above, the following model is proposed for the formation of a loess-tundra gley cycle caused by millennial-timescale climatic variations between ca 30 and 20 ka (Fig. 9):

Phase A – Cold, arid conditions. Typical loess deposition (coarser loess/high sedimentation rate).

Phase B – Continuing cold but more humid conditions. Progressive decrease in loess grain-size and sedimentation rate. Beginning of the development of an active layer, formation of ice wedges and cryoturbations in plateaux and in poorly drained areas.

Phase C – Interstadial (first part), more humid conditions, rapid warming and major decrease in the aeolian dynamics. Deepening in

Please cite this article in press as: Antoine, P., et al., Rapid and cyclic aeolian deposition during the Last Glacial in European loess: a high..., Quaternary Science Reviews (2009), doi:10.1016/j.quascirev.2009.08.001

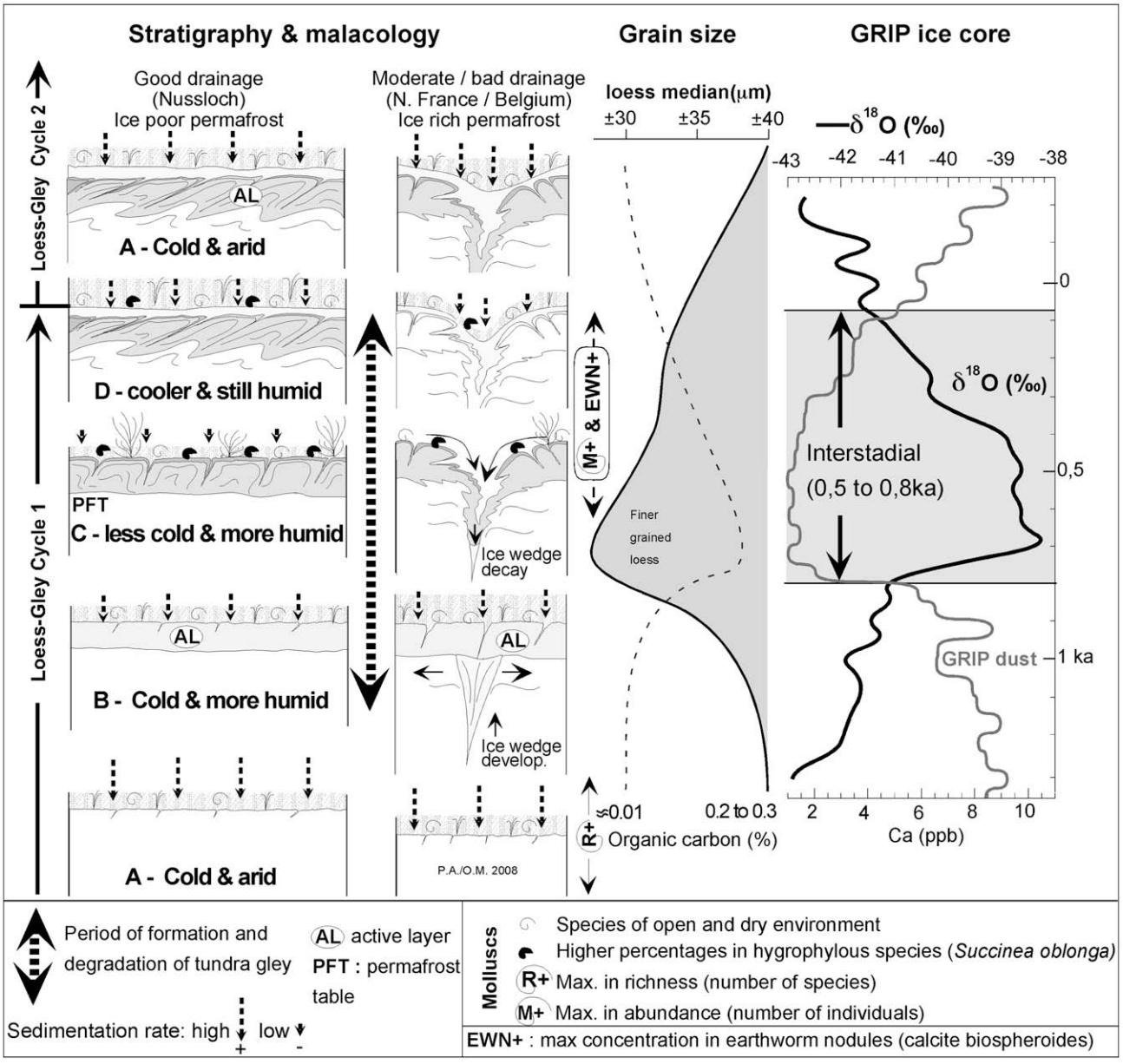

Fig. 9. Development model of a loess-tundra gley doublet during one D/O cycle (Ice-Core data: GIS 6, from Johnsen et al., 2001/Malacological data from Moine et al., 2008).

the active layer, strong reduction in the aeolian flux leading to the deposition of finer-grained loess. Higher levels of biological activity (vegetation, land snails, earthworms). Rapid rise in the proportion of the hygrophilous land snail *Succinella oblonga* that may be accompanied by an increase in abundance of all species. Start of decay of ice wedges and of the gelifluction of the upper part of the active layer. Local development of thermokarst processes.

Phase D – Interstadial (second part), cooler and more humid conditions. Final degradation of the tundra gley horizon. Gelifluction of the top of the active layer coinciding with the onset of a new phase of loess sedimentation (inclusion of pure loess between the "tongues" of geliflucted tundra gley). Decrease in the frequency of *Succinella oblonga,* while the total molluscan frequency remains still high.

Return to phase A – cold, arid and windier conditions. Sharp increase in deposition of coarser loess and start of a new loess–gley doublet. Rapid decrease in mollusc abundance and in the proportion of hygrophilous species.

6.2. Comparison between grain-size and magnetic susceptibility records

According to many studies, most of them performed on Chinese loess sequences, the highest values in magnetic susceptibility mainly result from the enrichment of ferromagnetic minerals (magnetite and maghemite) produced during pedogenesis (Zhou et al., 1990; Maher and Thompson, 1992; Heller and Evans, 1995) by bacterial (magnetotactic bacteria) activity within soil horizons (Maher and Taylor, 1988). This interpretation agrees with the results of MS measurements from Eemian and Early Weichselian loess–palaeosol sequences from Western Europe, including Nussloch (Antoine et al., 1999, 2001, 2003a).

In contrast, the cause of the main MS variations in the UPG loess sequence at Nussloch appears to be to the converse of this classical pedological explanation. This is because the MS maxima occur in loess and MS minima occur in tundra gley soils (Antoine et al., 2001). Similar observations showing high MS values within

unweathered loess have been published for Poland (Nawrocki et al., 1996), Siberia (Chlachula et al., 1998; Zander et al., 2003), and Alaska (Beget et al., 1990). In each case, the profiles were situated close to sources of fluvial silts and sands, in the same way as Nussloch is located close to the Rhine Valley. Nawrocki et al. (1996) suggest that the decrease in MS values in tundra gleys is partly related to the weathering of the magnetic minerals (magnetite to hematite), which is typical of water saturated soils. In contrast, Beget et al. (1990) suggest that the acceleration of the wind speed induces an increase in the amount of detrital magnetite in the loess being eroded from local source area consisting of dry braided river systems.

Considering the parallelism existing between MS at Nussloch and coarse silt percentage variations (clearly depicted by GSI variations), especially in the lower half part of the UPG loess sequence of P4 (Fig. 7), it is proposed that an increase in MS values (8–10 SI units) results from an enrichment in coarse, silt size (20–50 μm) detrital magnetic minerals. By comparison, measurements from the UPG loess of northern France, where no coarse detrital magnetic minerals have been found (Rousseau et al., 1994; Antoine et al., 1999), are definitely lower than in Nussloch. The high MS values in UPG loess are also associated with the lowest clay percentages, again suggesting a detrital origin for the MS signal.

The sources of coarse silt and associated magnetic grains are not obvious. The local substratum of the Kraichgau plateau around Nussloch is composed of Triassic limestones and marls, and Tertiary clays, which contain no coarse grain fractions. Likewise the surface sediments of the English Channel and of the southern North Sea, which are considered to be the main sources for the northwest-European loess sequences (Lautridou, 1985), have very low MS values (Rousseau et al., 1998, Antoine et al., 1999). In these circumstances, it is proposed that the ferromagnetic minerals, responsible for the high MS values in the UPG loess at Nussloch, probably originate from the braided river sediments of the Rhine Valley, which was dried-out and exposed to deflation during the Weichselian UPG. The silt and sand in the Nussloch UPG loess would therefore be mostly of local origin and the proximity of the source material would explain the exceptional thickness of the deposit.

The relationship between the aeolian sediments at Nussloch and the Rhine River braidplain is confirmed by the occurrence of fine sand layers within the UPG laminated loess units, and of coarse sands and fine gravels (up to 4–5 mm in diameter) within unit 13 (Fig. 2). All these strata are typical of sand dunes (±6 m in thickness) which formed close to P1 (Antoine et al., 2001); suggesting a local origin. More support for this interpretation is provided by the large Younger Dryas-aged dunes exposed near the city of Sandhausen, at the foot of the slope leading to the Nussloch site (Löscher and Haag, 1989; Antoine and Rousseau pers. obs.). The grain size and micromorphology of these aeolian sand facies are similar to those observed in the LPG dune (unit 13) of P1 profile and in the sandy beds from the UPG loess.

The source of the sediments at Nussloch indicates that the winds responsible for both deflation and transportation was blowing from the North to the Northwest, parallel with the main axis of the loess ridges (Fig. 1B). The presence of coarse silt and sandy loess layers also suggests saltation and periods of powerful wind activity from the N and NW transporting this coarser material at least over 3 km in distance and 90 m in elevation.

6.3. Sedimentation rates

According to ^{14}C and IRSL data from profile P2, the average sedimentation rate through the 10 m of UPG loess is about 1 mm yr^{-1} depending on the interval of uncertainty of the dates and is in accordance with the values used for the calculation of the loess Mass Accumulation Rates during MIS 2 in Western Europe (Frechen et al., 2003).

However, the occurrence of loess–gley doublets and of grain-size cycles throughout the Nussloch profiles implies millennial-timescale changes in loess deposition. Indeed, as the analysis of thin sections demonstrates, no pedogenesis and clay illuviation occurred within the tundra gleys (Antoine et al., 2001), the increase in the clay fraction is interpreted as the result of lower sedimentation rates and of a finer-grained aeolian input. In this case, it is estimated that a 50–80% reduction in the sedimentation rate occurred during each period of gley formation over a period of 0.2–0.8 ka per interstadial, based upon the Greenland ice-core chronology (Johnsen et al., 2001). Taking into account the error in the IRSL and OSL dates, the sedimentation rate during the formation of the tundra gleys is: ~0.70 mm yr^{-1} between the top of LB and the top of G2b, ~1.03 mm yr^{-1} between the top of G2b and ET and ~1.18 mm yr^{-1} between ET and the base of the topsoil (average: ±0.96–1.00 mm yr^{-1} for the whole UPG loess).

The general trend indicates that the sedimentation rate increased up the profile, especially in the upper 5 m. These rates are lower than those for the Late Wisconsinian loess in Nebraska, USA (Mason, 2001; Bettis et al., 2003; Rousseau et al., 2007b) or rates recorded during the present-day dust storms in the Chinese province of Gansu (Derbyshire et al., 1998). However, it is essential to note that sedimentation rates depend on a number of factors such as the availability of deflatable material, the distance from the source area, the wind strength in the context of the local topography and the surface characteristics of both source and depositional areas (humidity, roughness, vegetation).

The sedimentation rates proposed here are in agreement with the thickness of the individual fining-upward laminations described in part 5.1.1 which indicate >1 mm thick depositional events, a clear indication of rapid sedimentation. The UPG at Nussloch therefore records very short (dust storm-like) or secular scale climatic events.

With minimum sedimentation rates of 1 mm yr^{-1} (Antoine et al., 2001), these fluctuations indicate centennial events for coarser loess deposition. Unlike the main cycles, which are correlated with clear changes in the stratigraphical record, these sub-cycles often occur within apparently homogeneous loess.

Finally, the UPG loess from Nussloch records two short periods of arid climate conditions marked by the homogeneous loess units 22 and 38, which bracket a longer humid period (probably with more snow cover) characterised by laminated loess and tundra gley layers (units 24–34). These laminated loess strata formed between ca 30 and 23 ka, as found in other European sequences (Haesaerts, 1985, Huijzer and Vandenberghe, 1998). This age range agrees with the occurrence of more intense precipitation responsible for the maximum development of the Scandinavian ice sheet (Elverhøi et al., 1995; Svendsen et al., 2004). A maximum of aridity is emphasised within the upper homogeneous loess by $\delta^{13}C$ from loess organic carbon (Hatté et al., 2001a, Hatté and Guyot, 2005), mollusc assemblages (Moine et al., 2002, 2008) and the development of tenuous tundra gleys, especially at the level of the Eltviller Tuff around 21 ± 2 ka. The aridity coincides with the maximum wind intensity characterised by maxima in both the GSI and sand fractions.

6.4. Comparison with grain-size records from European loess series and dust records from Greenland ice cores

6.4.1. Grain-size records from European loess series

As studies on Weichselian loess sequences in Europe have been based mainly on stratigraphical correlation, palaeopedology

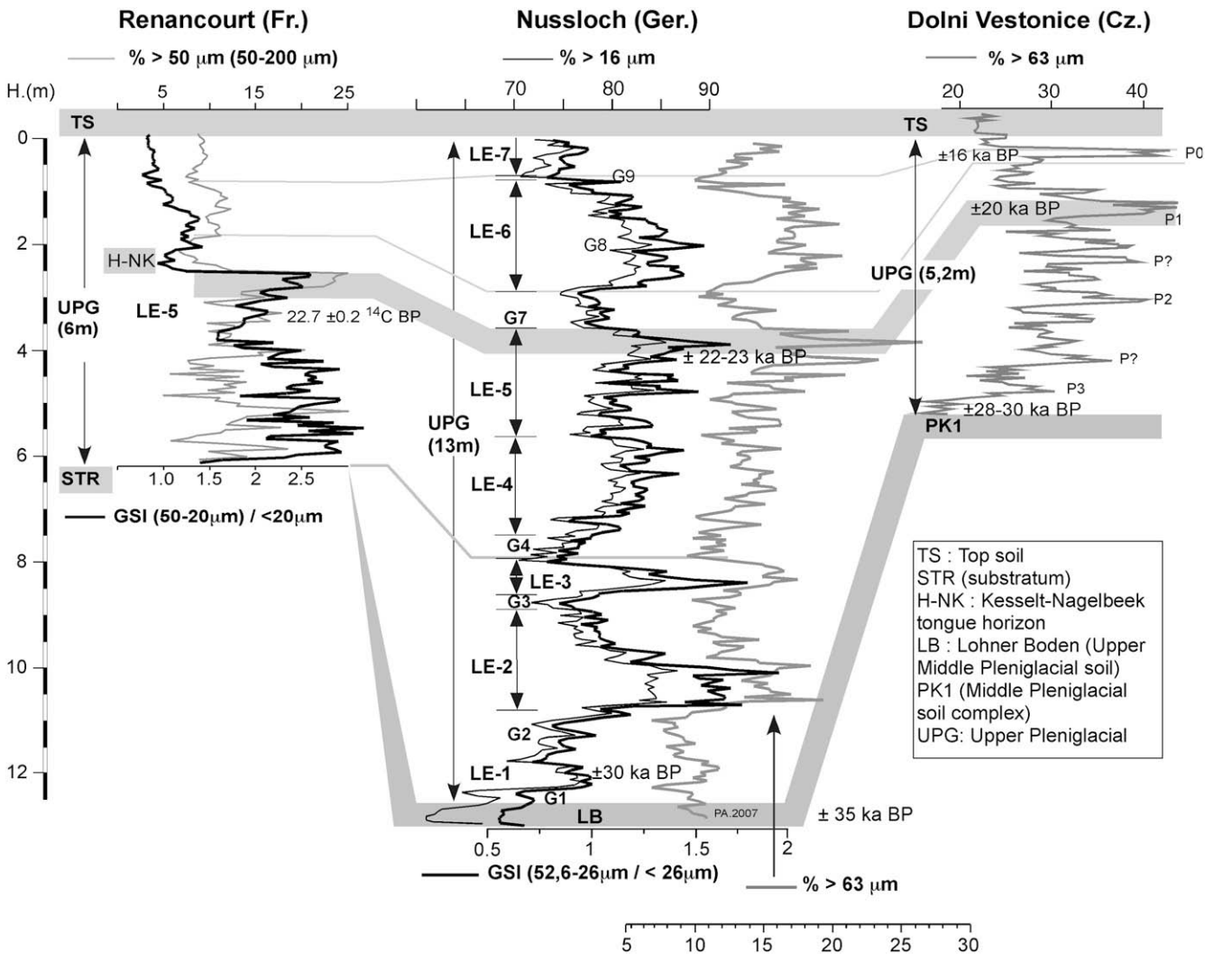

Fig. 10. Comparison between the grain-size variations within the UPG loess at Renancourt, Nussloch P4, Dolni Vestonice (Dolni Vestonice: according to Shi et al., 2003).

and periglacial process, only a few continuous high-resolution grain-size records are available for comparisons with those of Nussloch.

Starting in Western Europe, the record from Renancourt in the Somme basin (North France, Somme valley) provides a typical 7-m thick UPG loess profile (Fig. 10) (Antoine et al., EOLE unpublished data). For the grain-size study at this site, samples were taken at 5 cm intervals using the 'CCS' protocol developed in Nussloch (cf. Part 4. Grain size) and the analysis was performed using the sieve and pipette method. The stratigraphy of the Renancourt profile is simpler than that at Nussloch. It consists of two main calcareous loess units, a lower laminated unit and an upper homogeneous unit, separated by a well-marked tundra gley layer (H-NK), and capped by the reworked Bt horizon of the surface soil (Fig. 10). On the basis of stratigraphical evidence, the Renancourt profile is likely to represent only the upper half of the laminated loess LE-4 to LE-5, the tundra gley layer G7, and the homogenous loess LE-6 in Nussloch. The variations of both the GSI and fine sand percentage are parallel and show a two-fold pattern through this profile. The GSI increases rapidly from ca 1.5 at the base to ca 2.5–3 within the laminated loess unit, then rapidly falls to very low values (ca 1.0) in the tundra gley layer H-NK to remain very low (from ca 1.4 to 0.8) within the whole upper loess unit. Furthermore, the pattern of fine sand percentage variations from Renancourt and Nussloch profiles are similar and the range between the lowest and the highest values is about 20% in both curves.

These grain-size results from Renancourt show that the general coarsening of the loess, observed at Nussloch between the base of the UPG at ca 30 ka and the Last Glacial Maximum (±22 ka) below G7, is also well recorded towards the west. Moreover, the strongly asymmetrical shape that characterises the last cycle below the H-NK horizon in Renancourt is very close to that of LE-5 in Nussloch (Fig. 10). In addition, the shift between the Nussloch loess event LE-5 and G7, in both GSI and fine sand records, is sharper at Renancourt, where it is emphasised in the stratigraphy by a more developed tundra gley horizon (H-NK). On the basis of its position in the sequence and to the ^{14}C dating, this horizon is probably an equivalent of the Belgian Nagelbeek–Kesselt 'tongue horizon', that systematically occurs within the UPG sequence at about 22.0 ka ^{14}C BP, between the lower laminated loess (Hesbayen) and the upper homogeneous loess (Brabantian) (Lautridou and Sommé, 1974, Haesaerts et al., 1981). Among the west-European loess sections, and especially those from northern France and Belgium region, this grain-size shift above the Nagelbeek–Kesselt 'tongue horizon' has also been described in one other profile of the Somme Basin at Saint-Sauflieu (Antoine et al., 1999, and unpublished EOLE Data). This shift is associated with a marked change in the loess facies and to the well-known stratigraphical boundary between the two main

Please cite this article in press as: Antoine, P., et al., Rapid and cyclic aeolian deposition during the Last Glacial in European loess: a high..., Quaternary Science Reviews (2009), doi:10.1016/j.quascirev.2009.08.001

loess units of the Belgian UPG: the Hesbayen and Brabantian loess (Gullentops 1954; Haesaerts et al., 1981). In addition, a strong impoverishment in terrestrial mollusc faunas has been described within the homogeneous loess overlying the Nagelbeek–Kesselt 'tongue horizon' in both the Achenheim (Lautridou et al., 1985) and Nussloch sections (Moine et al., 2002, 2008).

Within the Belgian loess belt, a detailed grain-size record has been published by Vandenberghe et al. (1998), from the loess sequence at Kesselt, but the age of the deposits, dated using ^{14}C on mollusc shells, is strongly debated. Based on pedo-stratigraphical evidence (Juvigné et al., 1996) and TL dates (Van den Haute et al., 1998), these loess deposits should actually be allocated to the Late Saalian (MIS 6). Consequently, this grain-size record cannot be used for comparison, but shows that millennial-timescale grain-size variations not only typify the Last Glacial loess, they can also be recorded within Late Saalian sequences.

To extend the comparison eastwards into central Europe, the only available grain-size record is that of Dolni Vestonice in Czech Republic (Shi et al., 2003). This work is based on a discontinuous record of 5 cm interval samples and a LPS grain-size analysis undertaken without decarbonation, associated to a single TL date at the base of the UPG loess. The section is characterised by ca 5 m of apparently homogeneous loess, and a succession of four maxima in both the median grain size and fine sand percentage records (±15%: P0–P3). The lower maximum (P3) occurs just above the TL date at 28.2 ± 2.0 ka. The chronological allocation of the identified grain-size maxima P0–P3 with the Younger Dryas Stadial and Heinrich events H1, H2 and H3 by Shi et al. (2003), is based on a linear interpolation between the single TL date, obtained at the base of UPG and the lower boundary of topsoil supposed to be equivalent to MIS 2-1 boundary at ca 12 ka. However, numerous studies of European loess sequences demonstrated that loess sedimentation definitely stops at the end of the UPG at ca 16–15 ka before the first Lateglacial Interstadial (GRIP GI-e/Bølling, Björk et al., 1998) (Haesaerts, 1985; Rousseau et al., 1998; Antoine et al., 2003a,b; Frechen et al., 2003; Haesaerts et al., 2003;). Taking into account these observations, the youngest coarse maximum observed in Dolni Vestonice (P0) is more likely to be potentially equivalent to HE 1 at ca 15–16 ka, and P1 with HE 2 or with the coarse maxima observed in all the Nussloch profiles around 22–23 ka (Fig. 10).

Furthermore, even if the average sedimentation rates are very different (0.23–0.28 mm yr^{-1} in Dolni Vestonice vs. ≥1.00 mm yr^{-1} in Nussloch P4), the comparison between the two UPG grain-size records shows the same coarsening trend from ca 30 to 20 ka. This general trend is followed in both profiles by a strong decrease in the coarse particle content and then by a new increase at the top (LE-6/P0). Finally, the range of the fine sand fraction is also similar in both sections: 15% at NU-P4 and 20% at Dolni Vestonice. In this last record, the larger range could however be partly arise from the

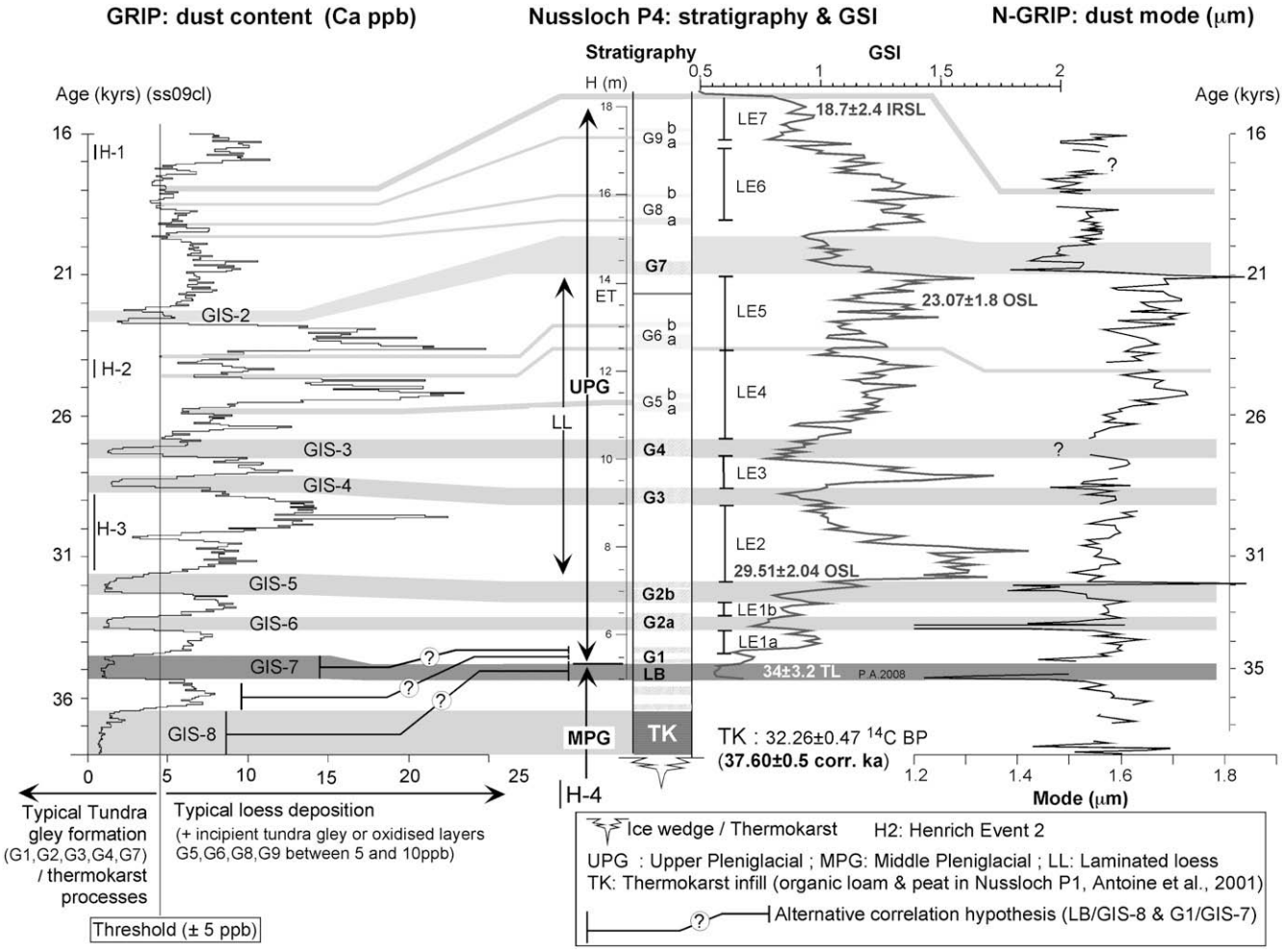

Fig. 11. Comparison between the grain-size index (GSI) through the UPG loess sequence at Nussloch and the variations of the dust content and dust median in the Greenland ice at GRIP and NGRIP (GRIP chronology based on Johnsen et al., 2001, NGRIP data from Ruth et al., 2006).

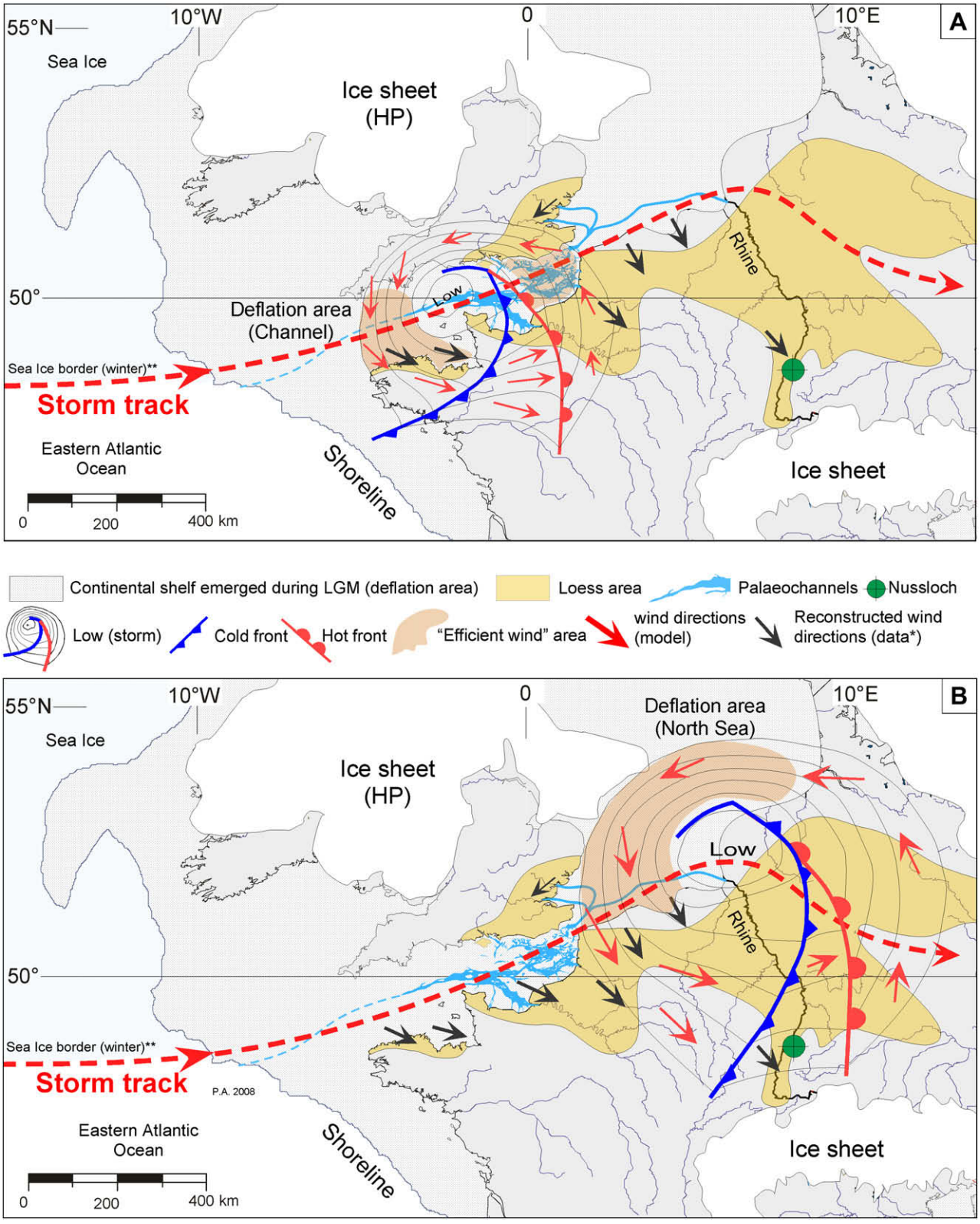

Fig. 12. Conceptual model linking the trajectory of North Atlantic low pressure centres, the location of sediment sources and loess depositional areas in Western Europe during the LGM. The loess area is taken from Antoine, et al., 2002, 2003b, LGM Ice sheets according to Renssen and Vandenberghe, 2003, The palaeochannel network is from Auffret et al., 1980, model of Atlantic low pressure centre according to Mayençon, 1989 and http://www.wetterzentrale.de, and reconstructed wind directions according to Lautridou, 1985, Antoine et al., 2003b and Vandenberghe et al., 2006. The 'efficient wind' area is defined as that part of the deflation area that is affected by the strong winds generated by the low pressure centre upwind of the depositional area. In Fig. 12a, when the low pressure is centred in the middle of the English Channel, two 'efficient wind' areas can be defined: one (EW-1) in the western Channel, north of the Brittany coast (NW to WNW winds) and one in the eastern Channel (S to SE winds). In Fig. 12b, when the low has moved to the south of the North Sea basin, a new 'efficient wind' area (EW-3) is defined in the southern North Sea (NW to N winds). This latter situation explains the deposition of aeolian sands on the southern and southeastern margins of the North Sea basin (the Cover Sands of Northern Belgium and the Netherlands), then of loess, further to the South (in Belgium and western Germany). At the same time, strong NW winds, associated with cold fronts, can remove particles from the local deflation areas (the dry braidplain of the River Rhine) and transport them a few kilometres to the southeast. At Nussloch, this local input of coarse silt and sands is likely at the origin of the very high sedimentation rate and of the 'greda morphology' that both characterises the UPG loess sequence.

Please cite this article in press as: Antoine, P., et al., Rapid and cyclic aeolian deposition during the Last Glacial in European loess: a high..., Quaternary Science Reviews (2009), doi:10.1016/j.quascirev.2009.08.001

absence of the coarse sand (>200 μm) removal before the grain-size analysis.

Further east, the best sequences available for comparison occur in the northern sandy loess zone of the Chinese Loess Plateau, where the sedimentation rates are, as in European sequences described, the highest during the deposition of the UPG loess, regionally termed L1-1 loess (Liu, 1985; Nugteren et al., 2004). Furthermore, the same coarsening trend occurs from a minimum at the base of L1-1 to a maximum at about 20 ka, associated to a similar range in fine sand (% >63 μm) grain-size variations: 20% in Huan Xian vs. 15% in Nussloch.

Despite these strong similarities, the sequences, separated by more than ten thousand kilometres, are nevertheless located within totally different climatic systems. A more detailed comparison between the Nussloch central European and Chinese loess sequences thus requires the thorough examination of other intermediate sequences in Eurasia (EOLE Project), such as in Serbia along the River Danube (Fuchs et al., 2007; Antoine et al., 2008), for example.

6.4.2. Dust records and D/O cycles from Greenland ice cores

The high-resolution investigation of grain-size in the Nussloch loess profiles allows recognition of rapid and cyclic variations in the distribution of the different grain-size fractions, especially for the GSI and the relative frequency of fine sand, that are both interpreted as proxies for aeolian dynamics.

Indeed, the higher the GSI ratio (coarser material), the higher the aeolian dynamics responsible for loess deposition, and consequently the greater is the sedimentation rate, as Nugteren et al. (2004) suggested for Chinese loess sequences. Conversely, low values of GSI correspond to a strong reduction in dust deposition leading to the stabilisation of the ground surface and to the development of a tundra gley. These results allowed the definition of a succession of seven phases of loess deposition (Loess Events: LE) and tundra gley soils (G) within the UPG loess at Nussloch between ca 34 and 17 ka (Fig. 7).

Taking into account the chronological framework established using the ^{14}C and OSL dates (Hatté et al., 2001b; Lang et al., 2003; Tissoux et al., in press) and both stratigraphical and grain-size patterns from profiles P3 and P4, a more detailed and robust correlation between the 'Loess Events' LE-1 to LE-7, defined by high GSI values, and the Greenland dust peaks recorded in GRIP, GISPII and NGRIP (GRIP Members, 1993; De Angelis et al., 1997; Johnsen et al., 2001; NGRIP Members, 2004; Andersen et al., 2006; Ruth et al., 2006) can be proposed for the interval ca 34–17 ka (Fig. 11). This result completes and strengthens the original correlation based only on the P2 data (Rousseau et al., 2002) and modified for P4 (Rousseau et al., 2007a).

In addition to this correlation, a schematic mechanism linking the sedimentation of the dust at the Greenland summit and in Nussloch has been produced. The first step represented by the numerical modelling of dust emissions from the deflation area is in progress at present (Sima et al., in press). The correspondence between these two different records implies the existence of a link between the variations in the aeolian dynamics over Western Europe and the atmospheric circulation over the North Atlantic area (Rousseau et al., 2007a). Indeed, it is likely that the increase in both frequency and intensity of the storms, implying strong NW to NNW winds, generated an enhancement of the deflation and of the high-altitude transport of silt particles from the emerged deflation area of the North Sea and Channel basins (distal input), in parallel with an enhancement in the local deflation of coarse loam and sand from European braided alluvial plains (local input) (Fig. 12). It can be also stressed that the huge increase in the loess depositional rate during MIS 2 is a general signature corresponding to a general phenomenon in the European loess series (Frechen, 1999; Frechen et al., 2003; Antoine et al., 1999; Rousseau et al. 1998, 2002; Haesaerts et al., 2003).

Based on the evidence from Nussloch, it is highly probable that the various D/O events have been recorded within the studied continental sequence (Rousseau et al., 2002, 2007a). Indeed, as proposed in Fig. 3, the climatic warming corresponding to the warm phases of the D/O events is associated with:

1) The development of tundra gley layers, indicating important increases in surface moisture (water-logging), resulting from the enhancement in the seasonal melting of the active layer.
2) A marked development of the vegetation (root tracks/organic carbon) and of the associated biological populations: very high abundances in molluscs (number of individuals) and in earthworms (0.5–1 mm calcite nodules) at the top of the tundra gley horizons.
3) A decrease of the permafrost during the rapid climatic warming characterising the first part of the interstadials, locally inducing thermokarst erosion in slope environments.

Studies of the organic geochemistry highlighted a comparable feature, with the occurrence of only C3 plants along the sequence, and more negative $\delta^{13}C$ values associated to wetter condition reconstructions during interstadial episodes (Hatté et al., 2001a; Hatté and Guyot, 2005).

Within the three profiles, and especially in P4, where the pedosedimentary budget is the highest, various soil horizons are clearly expressed. Their pedological facies vary from arctic brown soils at the base (Lohner Boden, unit, 20) to well expressed tundra gley horizons (Gelic Gleysols) within the lower two-thirds of the UPG loess, then to incipient gley horizons in the upper part of the profile. Considering the whole of the investigations undertaken in Nussloch, the impact of the D/O events, seen as the development of soil horizons, seems to be a function of the magnitude of the associated warming, and of the duration of the interstadials (see fig. 3 in Rousseau et al., 2007a) expressed in the marine and ice-core records (threshold effect, Fig. 11). Indeed, the comparison between the Greenland records and Nussloch series for the interval studied indicates that more intense and longer interstadials are expressed in the stratigraphy by well distinguished soil horizons, such as the Cambisol of unit 20 (arctic brown soil) underlying the base of the UPG sequence.

Conversely, shorter interstadials in Greenland ice cores are expressed in the terrestrial stratigraphy by a tundra gley horizon resulting from the deepening of the active layer (see part 6.1). Based on the detailed correlation presented in Fig. 11, the stratigraphical signature of these horizons (thickness, colour intensity, surface deformation cryoturbation/gelifluction) also seems to be linked to the duration and intensity of the interstadial: the strongest tundra gley horizons, such as G2, G3 or G4, characterises the longest interstadials (ca 0.8–0.3 ka), whereas only incipient gley horizons appear in response to very short (≤1 ka), and unlabelled oscillations, in the ice-core records. This hierarchy in the pedosedimentary response is also well-marked by the molluscan abundance, which depends on the corresponding warming intensity (D/O events 7–2) and increases in moisture (Moine et al., 2008). Molluscan richness cycles, i.e. variations in the number of species, also emphasise these alternations between loess and tundra gley during the UPG, the strongest decreases being associated with the moistest events.

Moreover, the comparison between the Greenland ice-core and the Nussloch sequences also shows that the intervals during which the aeolian sedimentation is coarser, as in units 24 and 34, indicating more intense aeolian dynamics, are penecontemporaneous with massive iceberg discharges in the North Atlantic Ocean (H3

Please cite this article in press as: Antoine, P., et al., Rapid and cyclic aeolian deposition during the Last Glacial in European loess: a high..., Quaternary Science Reviews (2009), doi:10.1016/j.quascirev.2009.08.001

and H2 events, Grousset, 2002). This reinforcement of the aeolian dynamics is associated with very poor vegetation indicated by $\delta^{13}C$ and reduced mollusc populations at Nussloch (Rousseau et al., 2002). It supports the recognition of episodes coeval to Heinrich events in the loess series (Rousseau et al., 2006). It could be argued that the intervals of fine grain-size values indicate a different origin than those of coarser size. However, such interpretation does not reject the assumption of variable winds, and so of different atmospheric patterns.

Finally, on the basis of the high-resolution grain-size and stratigraphical evidence from Nussloch, Renancourt and Dolni Vestonice, the general trend in grain-size observed within the European UPG loess series appears to be very close to that of the dust grain size in the NGRIP ice core. The terrestrial median grain size and the ice-core mode both show an increasing trend between ca 35 and 21 ka, which is followed by a rapid decrease at 21 ka, and then remains roughly stable but with lower values prevailing to the top of the records (NGRIP Members, 2004; Ruth et al., 2006).

This observation indicates the existence of a common process linking loess (grain-size and sedimentation rates) and dust (median and concentration) transportation and deposition at the scale of the whole North Atlantic and European region (Fig. 12).

7. Conclusions

The high-resolution analysis of the grain-size variations within the Upper Pleniglacial loess sequences at Nussloch, coupled with detailed stratigraphy, magnetic susceptibility, malacology, and luminescence and ^{14}C AMS dating lead to the following conclusions:

1 Grain-size variations through the three profiles analysed, and especially that of the coarse silt fraction expressed by the GSI ratio, and the fine sand percentage (>63 μm) allow definition of a cyclic succession (saw-tooth pattern) of tundra gley layers (G) and Loess Events (LE) following the detailed stratigraphical succession (seven LE-G doublets) between ca 34 and 17 ka.

2 These loess–gley successions result from cyclic variations in average wind intensity during periods of some thousand years to some centuries for the shorter ones. During periods of coarse loess deposition, the sedimentation rates are extremely high (>1 mm/ka). Taking in account all the ^{14}C and TL-OSL dates and the stratigraphical evidence, a correlation is proposed between the GSI maxima, indicating coarser loess deposition, and the main dust concentration peaks of the Greenland ice cores. Moreover, the general trends of both loess grain size and dust median in NGRIP show comparable variations. This correlation is reinforced by the demonstration of a hierarchy within the stratigraphical record, linking the type of soil (arctic brown soils/tundra gley/incipient gley) to the relative duration of the various Greenland interstadials (GIS). The Nussloch data thus reinforce the fundamentally discontinuous character of the loess sedimentation and support the apparent relationship between the loess sedimentation in Europe and global variations of the dust content of the atmosphere over Northern Hemisphere.

3 Taking into account the complete sedimentological, stratigraphical and biological evidence presented, a detailed model of loess-tundra gley doublets formation is proposed, showing that between ca 30 and 17 ka, the main tundra gley horizons as G2, G3, or G4, developed during the Interstadials of the D/O Cycles in response to weak loess sedimentation (low dust content in Greenland) and rapid warming. They are characterised by an enhancement in the seasonal melting of the active layer, and the development of the vegetation and biological communities.

4 Contrary to what is generally observed in European loess profiles, magnetic susceptibility variations within the UPG loess are not controlled by pedological processes but by the variations in the amount of detrital magnetite. Within the tundra gley layers, the MS signal is abnormally low owing to the weathering of the magnetic minerals during periods of water-logging. The parallelism between the variations in magnetic susceptibility and the coarse silt fraction shows that during the UPG the allochtonous sedimentation was locally disturbed by a local input characterised by coarser grain size and a greater abundance in magnetic minerals.

5 The analysis of the laminated loess indicates very high frequency variability within this facies, typical of the 30–20 ka time interval in the west-European loess series. Based on the Nussloch data, it is interpreted, as the result of numerous and intense dust storms during the UPG, were able to rework and transport coarse sand grains from the braided alluvial plain of the Rhine.

6 Compared with other European loess profiles, the Nussloch loess sequence provides the most detailed record of the aeolian sedimentation during the UPG in Europe. Even though strong similarities exist between the global trends of the grain-size records from Nussloch, and those from other European and Chinese sequences, a detailed comparison at the Eurasian continental scale still requires many more intermediate sequences to be investigated.

7 Finally, by combining the different studies, the discontinuous character of loess deposition in this area supported by the differing proxies obtained is address. A mechanism is proposed to explain the dust transport from both local (braided rivers) and very distant (continental shelf) sources, involving the trajectories of North Atlantic low pressure centres over Western Europe during the LGM, and contributing to the exceptionally thick loess deposits found at Nussloch.

Acknowledgements

The authors thank Dr. M. Löscher for his help and interesting discussions during field work, the Heidelberger Zement Company for the access to their quarry, their interest in loess research and the preservation of profile P4, U. Ruth for providing the data from the NGRIP dust record, Dr. N. Limondin-Lozouet for the review of the first draft of the manuscript, Pr. Jim Rose for his valuable comments and Pr. Phil Gibbard for the final review of the manuscript. These investigations have been undertaken under the framework of the European Project BIMACEL focusing on the high-resolution study of the loess record of the last climatic cycle, of the CNRS ECLIPSE "EOLE" project focusing on the 30–15 ka interval and of ANR project ANR-08-BLAN-0227 ACTES. This paper is LDEO contribution 7280 and LSCE contribution n° 4040.

References

Andersen, K.K., Svensson, A., Johnsen, S.J., Rasmussen, S.O., Bigler, M., Röthlisberger, R., Ruth, R., Siggaard-Andersen, M.-L., Steffensen, J.-P., Dahl-Jensen, D., Vinther, B.M., Clausen, H.B., 2006. The Greenland ice core chronology 2005, 15–42 ka. Part 1: constructing the time scale. Quaternary Science Reviews 25, 3246–3257.

Antoine, P., Rousseau, D.D., Lautridou, J.P., Hatté, C., 1999. Last interglacial–glacial climatic cycle in loess-palaeosol successions of north-western France. Boreas 28, 551–563.

Antoine, P., Rousseau, D.D., Zöller, L., Lang, A., Munaut, A.V., Hatté, C., Fontugne, M., 2001. High resolution record of the last interglacial–glacial cycle in the Nussloch loess–palaeosol sequences, Upper Rhine Area Germany. Quaternary International 76–77, 211–229.

Antoine, P., Rousseau, Hatté, C., Zöller, L., Lang, A., Fontugne, M., Moine, O., 2002. Événements éoliens rapides en contexte loessique: l'exemple de la séquence du

Pléniglaciaire supérieur weichselien de Nussloch (Vallée du Rhin-Allemagne). Quaternaire 13, 3–4. 199–208.
Antoine, P., Bahain, J.-J., Debenham, N., Frechen, M., Gauthier, A., Hatté, C., Limondin-Lozouet, N., Locht, J.-L., Raymond, P., Rousseau, D.-D., 2003a. Nouvelles données sur le Pléistocène du Nord du Bassin Parisien: les séquences loessiques de Villiers-Adam (Val d'Oise, France). Quaternaire 14, 219–235.
Antoine, P., Catt, J., Lautridou, J.P., Sommé, J., 2003b. The loess and coversands of Northern France and Southern England. Journal of Quaternary Science 18, 309–318.
Antoine, P., Rousseau, D.D., Fuchs, M., Hatté, C., Markovic, S.B., Jovanovic, M., Gaudenyi, T., Moine, O., Rossignol, J., 2008. High resolution record of the last climatic cycle in the Southern Carpathian basin at Surduk (Vojvodina, Serbia). Quaternary International 198, 19–36.
Auffret, J.P., Alduc, D., Larsonneur, C., Smith, A.J., 1980. Cartographie du paléoréseau des paléovallées et de l'épaisseur des formations superficielles meubles de la Manche orientale. Annales de l'Institut Océanographique, Paris 56 (S), 21–35.
Bard, E., Arnold, M., Hamelin, B., Tisnérat-Laborde, N., Cabioch, G., 1998. Radiocarbon calibration by means of mass spectrometric $^{230}Th/^{234}U$ and ^{14}C ages of corals. An updated data base including samples from Barbados. Radiocarbon 40 (3), 1085–1092.
Beget, J.E., Stone, D.B., Hawkins, D.B., 1990. Paleoclimatic forcing of magnetic susceptibility variations in Alaska loess during the late Quaternary. Geology 18, 40–43.
Bente, B., Löscher, M., 1987. Sedimentologishe, pedologishe und stratigraphishe Unterschungen an Lössen südlich Heidelberg. Göttinger geogr. Abh 84, 9–17.
Bettis, E.A., Mason, J.P., Swinehart, J.B., Miao, X.D., Hanson, P.R., Goble, D.B., Loope, P.M., Jacobs, R.J., Roberts, H.M., 2003. Cenozoic eolian sedimentary systems of the USA midcontinent. In: Easterbrook, D.J. (Ed.), Quaternary Geology of the United States, INQUA 2003 Field Guide Volume. Desert Research Institute, Reno, pp. 195–218.
Bibus, E., 1980. Zur Relief-, Boden- und Sedimententwicklung am unteren Mittelrhein. Frankfurter geowiss. Arb. D1, 296.
Bibus, E., Frechen, M., Kösel, M., Rähle, W., 2007. Das jungpleistozäne Lössprofil von Nussloch (SW-Wand) im Aufschluss der Heidelberger Zement AG. Eiszeitalter und Gegenwart 56–4, 227–255.
Björk, S., Walker, M.J.C., Cwynar, L.C., Johnsen, S., Knudsen, K.-L., Lowe, J.J., Wohlfarth, B., INTIMATEMembers, 1998. An event stratigraphy for the last termination in the North Atlantic region based on the Greenland ice-core record: a proposal by the INTIMATE group. Journal of Quaternary Science 13, 283–292.
Boenigk, W., Frechen, M., 2006. The Pliocene and Quaternary fluvial archives of the Rhine system. Quaternary Science Reviews 25, 550–574.
Bond, G., Broecker, W., Lotti, R., McManus, J., 1993. Abrupt colour changes in isotope stage 5 in North Atlantic deep-sea cores: implications for rapid change of climate-driven events. In: Kukla, G.J., Went, E. (Eds.), Start of a Glacial. Springer-Verlag, Heidelberg, pp. 185–205. Series I: Global Environmental Change.
Brunnacker, K., 1986. Quaternary stratigraphy in the lower Rhine area and northern Alpine foothills. Quaternary Science Reviews 5, 373–379.
Chlachula, J., Evans, M.E., Rutter, N.W., 1998. A magnetic investigation of a late Quaternary loess/palaeosol record in Siberia. Geophysical International Journal 132, 128–132.
De Angelis, M.R., Steffensen, J.P., Legrand, H.B., Clausen, H.B., Hammer, C.U., 1997. Primary aerosol (sea salt and soil dust) deposited in Greenland ice during the last climatic cycle: comparison with east Antarctic records. Journal of Geophysical Research 102, 26681–26698.
Derbyshire, E., Meng, X., Kemp, R., 1998. Provenance, transport and characteristics of modern aeolian dust in western Gansu province, China, and interpretation of the Quaternary loess record. Journal of Arid Environments 39, 497–516.
Dolecki, L., 1986. Differentiation of grain size of the Vistulian loesses on the Grzeda Horodelska Plateau (SE Poland). In: Maruszczak, H. (Ed.), Problems of the Stratigraphy and Paleogeography of Loesses. Maria Curie-Sklodowska University, Canada, pp. 165–178.
Ding, Z.L., Ren, J.Z., Yang, L.S., Liu, T.S., 1998. Climatic instability during the Penultimate glaciation: evidence from two high-resolution loess records. China Journal of Geophysical Research 104, 123–132.
Ding, Z.I., Rutter, N.W., Sun, J.M., Yang, S.L., Liu, T.S., 2000. Re-arrangement of atmospheric circulation at about 2.6 Ma over northern China: evidence from grain size records of loess–palaeosol and red clay sequences. Quaternary Science Reviews 19, 547–558.
Ding, Z.L., Derbyshire, E., Yang, S.L., Yu, Z.W., Xiong, S.F., Liu, T.S., 2002. Stacked 2.6-Ma grain size record from the Chinese loess based on five sections and correlation with the deep-sea $\delta^{18}O$ record. Paleoceanography 17, 5.1–5.21.
Elverhøi, A., Andersen, E.S., Dokken, T., Hebbeln, D., Spielhagen, R., Svendsen, J.I., Sørflaten, M., Rørnes, A., Hald, M., Forsberg, C.F., 1995. The growth and decay of the late Weichselian ice sheet in western Svalbard and adjacent areas based on provenance studies of marine sediments. Quaternary Research 44, 303–316.
Fang, X.M., Li, J.J., Van der Voo, R., 1999. Rock magnetic and grain size evidence for intensified Asian atmospheric circulation since 800,000 years B.P. related to Tibetan uplift. Earth and Planetary Science Letters 165, 129–144.
Frechen, M., 1999. Upper Pleistocene loess stratigraphy in Southern Germany. Quaternary Geochronology 18, 243–269.
Frechen, M., Oches, E.A., Kohfeld, K.E., 2003. Loess in Europe-mass accumulation rates during the last glacial period. Quaternary Science Reviews 22, 1835–1857.
Fuchs, M., Rousseau, D.D., Antoine, P., Hatté, C., Gauthier, C., 2007. Chronology of the last climatic cycle (upper Pleistocene) of the Surduk loess sequence, Vojvodina, Serbia. Boreas 10, 1–8.
GRIP Members, 1993. Climate instability during the last interglacial period recorded in the GRIP ice-core. Nature 364, 203–207.
Grousset, F., 2002. Les changements abrupts du climat depuis 60 000ans. Quaternaire 12, 203–211.
Gullentops, F., 1954. Contribution à la chronologie du Pléistocène et des formes de relief en Belgique. Mémoire de l'Institut de Géologie, Université de Louvain XVIII, 125–252.
Haesaerts, P., 1985. Les loess du Pléistocène Supérieur en Belgique; comparaison avec les séquences de l'Europe Centrale. Bulletin de l'Association Française pour l'Etude du Quaternaire 22, 105–115.
Haesaerts, P., Van Vliet-Lanoë, B., 1974. Compte-rendu de l'excursion du 25 mai 1974 consacrée à la stratigraphie des limons aux environs de Mons. Annales de la Société Géologie et de Paléontologie 978, 547–560.
Haesaerts, P., Van Vliet-Lanoë, B., 1981. Phénomènes périglaciaires et sols fossiles observés à Maisières-Canal, à Harmignies et à Rocourt. Biultyn peryglacalny 28, 291–324.
Haesaerts, P., Juvigné, E., Kuyl, O., Mücher, H., Roebroeks, W., 1981. Compte rendu de l'excursion du 13 Juin 1981, en Hesbaye et au Limbourg Néerlandais, consacrée à la chronostratigraphie des loess du Pléistocène supérieur. Annales de la Société Géologique de Belgique 104, 223–240.
Haesaerts, P., Borziak, I., Chirica, V., Damblon, F., Koulakovska, L., Van der Plicht, J., 2003. The east-Carpathian loess record: a reference for the middle and late Pleniglacial stratigraphy in Central Europe. Quaternaire 14 (3), 163–188.
Hatté, C., Fontugne, M., Rousseau, D.D., Antoine, P., Zöller, L., Tisnéra-Laborde, N., Bentaleb, I., 1998. ^{13}C Variations of loess organic matter as a record of the vegetation response to climatic changes during the Weichselian. Geology 26 (7), 583–586.
Hatté, C., Antoine, P., Fontugne, M., Rousseau, D.D., Tisnéra-Laborde, N., Zöller, L., 1999. New chronology and organic matter $\delta^{13}C$ paleoclimatic significance of Nussloch loess sequence (Rhine Valley, Germany). Quaternary International 62, 85–91.
Hatté, C., Antoine, P., Fontugne, M., Lang, A., Rousseau, D.D., Zöller, L., 2001a. $\delta^{13}C$ of loess organic matter as a potential proxy for paleoprecipitation. Quaternary Research 55, 33–38.
Hatté, C., Pessenda, L.C., Lang, A., Paterne, M., 2001b. Development of accurate and reliable ^{14}C chronologies for loess deposits: application to the loess sequence of Nussloch (Rhine Valley, Germany). Radiocarbon 43 (2B), 611–618.
Hatté, C., Guyot,, J., 2005. Paleoprecipitation reconstruction by inverse modelling using the isotopic signal of loess organic matter: application to the Nussloch loess sequence (Rhine Valley, Germany). Climate Dynamics 25, 315–327.
Heller, F., Evans, M.E., 1995. Loess magnetism. Reviews of Geophysics 33 (2), 211–240.
Huijzer, B., Vandenberghe, J., 1998. Climatic reconstruction of the Weichselian Pleniglacial in northwestern and central Europe. Journal of Quaternary Science 13 (5), 391–417.
Johnsen, S.J., Dahl-Jensen, D., Gundestrup, N., Steffensen, J.P., Clausen, H.B., Miller, H., Masson-Delmotte, V., Sveinbjörnsdottir, A.E., White, J., 2001. Oxygen isotope and palaeotemperature records from six Greenland ice-core stations: Camp Century, Dye-3, GRIP, GISP2, Renland and NorthGRIP. Journal of Quaternary Science 16, 299–307.
Juvigné, E., Semmel, A., 1981. Un tuf volcanique semblable à l'Eltviller Tuff dans les loess de Hesbaye et du Limbourg néerlandais. Eiszeitalter und Gegenwart 31, 83–90.
Juvigné, E., Haesaerts, P., Metsdagh, H., Balescu, S., 1996. Révision du stratotype loessique de Kesselt (Limbourg, Belgique). Comptes Rendus de l'Académie des Sciences, Paris, série IIa 323, 801–807.
Konert, M., Vandenberghe, J., 1997. Comparison of laser grain size analysis with pipette and sieve analysis: a solution for the underestimation of the clay fraction. Sedimentology 44, 523–535.
Lang, A., Hatté, C., Rousseau, D.-D., Antoine, P., Fontugne, M., Zöller, L., Hambach, U., 2003. High-resolution chronologies for loess: comparing AMS ^{14}C and optical dating results. Quaternary Science Reviews, Quaternary Geochonology 22, 953–959.
Lautridou, J.-P., 1985. Le cycle périglaciaire pléistocène en Europe du Nord-Ouest et plus particulièrement en Normandie. Thèse es Sciences, Univ. Caen, Centre de Géomorphologie Caen, 908 pp.
Lautridou, J.P., Sommé, J., 1974. Les loess et les provinces climato-sédimentaires du Pléistocène supérieur dans le Nord-Ouest de la France. Bulletin de l'Association Française pour l'Étude du Quaternaire 11, 237–241.
Lautridou, J.P., Sommé, J., Heim, J., Puisségur, J.J., et Rousseau, D.D., 1985. La stratigraphie des lœss et formations fluviatiles d'Achenheim (Alsace): nouvelles données bioclimatiques et corrélations avec les séquences pléistocènes de la France du Nord-Ouest. Bulletin de l'Association Française pour l'Etude du Quaternaire 22, 125–132.
Léger, M., 1990. Loess landforms. Quaternary International 7/8, 53–61.
Liu, T.S. (Ed.), 1985. Loess and Environment. Ocean Press, Beijing, China, 251 pp.
Löscher, M., Haag, T., mit einem Beitrag von K. Münzing, 1989. Zum Alter der Dünen im nördlichen Oberrheingraben und zur Genese ihrer Baenderparabraunerden. Eiszeitalter und Gegenwart 39, 98–108. Hannover.
Maher, B.A., Taylor, R.M., 1988. Formation of ultrafine-grained magnetite in soils. Nature 336, 368–370.
Maher, B., Thompson, R., 1992. Paleoclimatic significance of the mineral magnetic record of the Chinese loess and paleosols. Quaternary Research 37, 155–170.

Please cite this article in press as: Antoine, P., et al., Rapid and cyclic aeolian deposition during the Last Glacial in European loess: a high..., Quaternary Science Reviews (2009), doi:10.1016/j.quascirev.2009.08.001

Mason, J.A., 2001. Transport direction of Peoria loess in Nebraska and implications for loess sources on the Central Great Plains. Quaternary Research 56, 79–86.
Mayençon, R., 1989. Météorologie marine. iN: Ouest-France (Ed.), 190 pp.
Moine, O., Rousseau, D.D., Antoine, P., Hatté, C., 2002. Mise en évidence d'événements climatiques rapides par les faunes de mollusques terrestres des loess weichseliens de Nussloch (Allemagne). Quaternaire 13 (3–4), 209–218.
Moine, O., Rousseau, D.D., Antoine, P., 2005. Terrestrial mollucan records of Weichselian lower and middle Pleniglacial climatic changes from Nussloch loess series (Rhine valley, Germany): the impact of local factors. Boreas 34, 363–380.
Moine, O., Rousseau, D.-D., Antoine, P., 2008. The impact of Dansgaard-Oeschger cycles on the loessic environment and malacofauna of Nussloch (Germany) during the upper Weichselian. Quaternary Research 70 (1), 91–104.
Nawrocki, J., Wojcik, A., Bogucki, A., 1996. The magnetic susceptibility record in the Polish and western Ukrainian loess–palaeosol conditioned by palaeoclimate. Boreas 25, 161–169.
NGRIP Members, 2004. High resolution climate record of the northern Hemisphere reaching into the last glacial interglacial period. Nature 431, 147–151.
Nugteren, G., Vandenberghe, J., van Huissteden, K., Zhisheng, A., 2004. A Quaternary climate record based on grain size analysis from the Luochuan loess section on the Central Loess Plateau, China. Global and Planetary Change 41, 167–183.
Paillard, D., Labeyrie, L., Yiou, P., 1996. Macintosh program performs time-series analysis. Eos Transactions AGU 77, 379.
Porter, S., An, Z., 1995. Correlation between climate events in the North Atlantic and China during the last glaciation. Nature 375, 305–308.
Reimer, P.J., Baillie, M.G.L., Bard, E., Bayliss, B., Beck, J.W., Bertrand, C., Blackwell, P.G., Buck, C.E., Burr, G., Cutler, K.B., Damon, P.E., Edwards, R.L., Fairbanks, R.G., Friedrich, M., Guilderson, T.P., Hughen, K.A., Kromer, B., McCormac, M.G., Manning, S., Bronk, C., RamseyReimer, R.W., Remmele, S., Southon, J.R., Stuiver, M., Talamo, S., Taylor, F.W., van der Plicht, J., Weyhenmeyer, C.E., 2004. IntCal04 terrestrial radiocarbon age calibration, 0–26 kyr BP. Radiocarbon 46 (3), 1029–1058.
Renssen, H., Vandenberghe, J., 2003. Investigation of the relationship between permafrost distribution in NW Europe and extensive winter sea-ice cover in the North Atlantic Ocean during the cold phases of the last glaciation. Quaternary Science Reviews 22, 209–223.
Rousseau, D.D., Soutarmin, N., Gaume, L., Antoine, P., Lang, M., Lautridou, J.P., Sommé, J., Zöller, L., Lemeur, I., Meynardier, L., Fontugne, M., Wintle, A., 1994. Histoire du Dernier cycle climatique enregistrée dans la séquence loessique d'Achenheim (Alsace, France), à partir de la susceptibilité magnétique. Comptes Rendus de l'Académie des Sciences, Paris 319 (II), 551–558.
Rousseau, D.D., Zöller, L., Valet, J.P., 1998. Late Pleistocene climatic variations at Achenheim, France, based on a magnetic susceptibility and TL chronology of loess. Quaternary Research 49, 255–263.
Rousseau, D.-D., Antoine, P., Hatté, C., Lang, A., Zöller, L., Fontugne, M., Ben Othman, D., Luck, J.-M., Moine, O., Labonne, M., Bentaleb, I., Jolly, D., 2002. Abrupt millenial climatic changes from Nussloch (Germany) Upper Weichselian eolian records during the last glaciation. Quaternary Science Reviews 21, 1577–1582.
Rousseau, D.-D., Kukla, G., Mac Manus, J., 2006. What is what in the ice and the ocean? Quaternary Science Reviews 25, 2025–2030.
Rousseau, D.-D., Sima, A., Antoine, P., Hatté, C., Lang, A., Zöller, L., 2007a. Link between European and North-Atlantic abrupt climate changes over the last glaciation. Geophysical Research Letters 34, L22713. 1029/2007/GL031716.
Rousseau, D.D., Antoine, P., Kunesch, S., Hatté, C., Rossignol, J., Lang, A., Packman, S., 2007b. Evidence of cyclic dust deposition in the US Great plains during the last deglaciation from the high-resolution analysis of the Peoria loess in the Eustis sequence (Nebraska, USA). Earth and Planetary Science Letters 262, 159–174.
Ruth, U., Wagenbach, D., Steffensen, J.-P., Bigler, M., 2006. Continuous record of microparticle concentration and size distribution in the central Greenland NGRIP ice core during the lastglacial period. Journal of Geophysical Research 108, 4098.
Sabelberg, U., Löscher, M., 1978. Neue Beobachtungen zur Würmlöss-Stratigraphie südlich Heidelberg. In: Fink, J. (Ed.), Festschr Wien, Hirt.
Semmel, A., 1997. Referenzprofile des Würmlösses im Rhein-Main-Gebeit. Jber. Wetterau. Ges. ges. Naturkunde 148, 37–47.
Schirmer, W., 2000. Rhein loess, ice cores and deep sea cores during MIS 2–5. Zeitschrift der Deutschen Geologischen Gesellschaft 151, 309–332.
Shi, C., Zhu, R., Glass, B.P., Liu, Q., Zema, A., Suchy, V., 2003. Climate variations since the last interglacial recorded in Czech loess. Geophysical Research Letters 30 (11), 16-1–16-4.
Sima, A., Rousseau, D.-D., Kageyama, M., Ramstein G., Schulz, M., Balkansky, Y., Antoine, P., Dulac, F., Hatté, C. North-Atlantic millennial-timescale variability imprint on Western European loess deposits: a modeling study. Quaternary Science Reviews, in press.
Sommé, J., Paepe, R., Lautridou, J.P., 1980. Principes, méthodes et système de la stratigraphie du Quaternaire dans le Nord-Ouest de la France et la Belgique. In: Problèmes de stratigraphie quaternaire en France et dans les pays limitrophes. Supplément au Bulletin de l'Association Française pour l'Etude du Quaternaire NS-1, pp. 148–162.
Sommé, J., Lautridou, J.P., Heim, J., Maucorps, J., Puisségur, J.J., Rousseau, D.D., Thévenin, A., Van Vliet-Lanoë, B., 1986. Le cycle climatique du Pléistocène supérieur dans les loess d'Alsace à Achenheim. Supplément au Bulletin de l'Association Française pour l'Etude du Quaternaire 23, 97–104.
Svendsen, J.I., Alexanderson, H., Astakhov, V.I., Demidov, I., Dowdeswell, J.A., Funder, S., Gataullin, V., Henriksena, M., Hjort, C., Houmark-Nielsen, M., Hubberten, H.W., Olfsson, I., Jakobsson, M., Kjær, K.H., Larsen, E., Lokrantz, H., Pekka Lunkka, J., Lyså, A., Mangerud, J., Matiouchkov, A., Murray, A., Mölleri, P., Niessen, F., Nikolskaya, O., Polyak, L., Saarnisto, M., Siegert, M., Spielhagen, R.F., Stein, R., 2004. Late Quaternary ice sheet history of northern Eurasia. Quaternary Science Reviews 23, 1229–1271.
Tissoux, H., Valladas, H., Voinchet, P., Reyss, J.L., Mercier, N., Falguères, C., Bahain, J.J., Zöller, L., Antoine, P. OSL and ESR studies of aeolian quartz sediments from the upper Pleistocene loess sequence of Nussloch (Germany). Quaternary Geochronology, in press. doi:10.1016/j.quageo.2009.03.009 Special Issue LED, 2008.
Vandenberghe, J., An, Z., Nugteren, G., Huayu, L., Van Huissteden, K., 1997. New absolute time scale for the Quaternary climate in the Chinese loess region by grain-size analysis. Geology 25 (1), 35–38.
Vandenberghe, J., Huijzer, B., Mücher, H., Laan, W., 1998. Short climatic oscillations in a western European loess sequence (Kesselt, Belgium). Journal of Quaternary Science 13, 471–485.
Vandenberghe, J., Nugteren, G., 2001. Rapid climatic changes recorded in loess next term successions. Global and Planetary Change 28, 1–9.
Vandenberghe, J., Renssen, H., van Huissteden, K., Nugteren, G., Konert, M., Lu, H., Dodonov, A., Jan-Buylaert, P., 2006. Penetration of Atlantic westerly winds into Central and East Asia. Quaternary Science Reviews 25, 2380–2389.
Van den Haute, P., Vancraeynest, L., de Corte, F., 1998. The Late Pleistocene loess deposits and palaeosols of eastern Belgium: new TL age determinations. Journal of Quaternary Science 13, 487–497.
Van Vliet-Lanoë, B., 1987. Le rôle de la glace de ségrégation dans les formations superficielles de l'Europe du Nord-Ouest. Thèse de Doctorat d'Etat, Université Paris I, 864 pp.
Xiao, J., Porter, S.C., An, Z., Kumai, H., Yoshikawa, S., 1995. Grain size of quartz as an indicator of winter monsoon strength on the Loess Plateau of Central China during the last 130 000 yr. Quaternary Research 43, 22–29.
Zander, A., Frechen, M., Zykina, V., Boenigk, W., 2003. Luminescence chronology of the upper Pleistocene loess record at Kurtak in middle Siberia. Quaternary Science Reviews 22, 999–1010.
Zhou, L.P., Oldfield, F., Wintle, A.G., Robinson, S.G., Wang, J.T., 1990. Partly pedogenic origin of magnetic variations in Chinese loess. Nature 346, 737–739.
Zöller, L., Stremme, H.E., Wagner, G.A., 1988. Thermolumineszenz-Datierung an Löss-Paläoboden-Sequenzen von Nieder-, Mittle-und Obberhein. Chemical Geology: Isotope Geoscience Section 73, 39–62.
Zöller, L., Wagner, G., 1990. Thermoluminescence dating of loess-recent developments. Quaternary International 7/8, 119–128.

Please cite this article in press as: Antoine, P., et al., Rapid and cyclic aeolian deposition during the Last Glacial in European loess: a high..., Quaternary Science Reviews (2009), doi:10.1016/j.quascirev.2009.08.001